

In presenting the dissertation as a partial fulfillment of the requirements for an advanced degree from the Georgia Institute of Technology, I agree that the Library of the Institute shall make it available for inspection and circulation in accordance with its regulations governing materials of this type. I agree that permission to copy from, or to publish from, this dissertation may be granted by the professor under whose direction it was written, or, in his absence, by the Dean of the Graduate Division when such copying or publication is solely for scholarly purposes and does not involve potential financial gain. It is understood that any copying from, or publication of, this dissertation which involves potential financial gain will not be allowed without written permission.

A handwritten signature in dark ink, appearing to be "J. S. ...", is written across the middle of the page.

3/17/65

b

THE MULTILAYER ADSORPTION OF KRYPTON
ON HEXAGONAL BORON NITRIDE

A THESIS

Presented to
The Faculty of the Graduate Division
by
Alvin Charles Levy

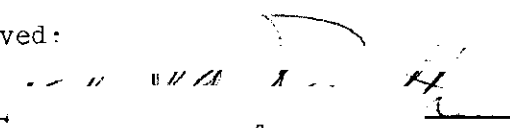
In Partial Fulfillment
of the Requirements for the Degree
Master of Science in Chemistry

Georgia Institute of Technology

August, 1966

THE MULTILAYER ADSORPTION OF KRYPTON
ON HEXAGONAL BORON NITRIDE

Approved:


Chairman

Date approved by Chairman: 15 June 66

DEDICATION

I dedicate this thesis to my wife, Joan, without whose encouragement and understanding its completion would not have been possible.

ACKNOWLEDGMENTS

The author gratefully acknowledges the assistance, advice, and encouragement given to him by Dr. Robert A. Pierotti, the director of this research. The author also wishes to thank Mr. James J. McAlpin for his help rendered on many matters, and Mr. Reginald Ramsey and Mr. Robert Smallwood for their helpful and sometimes entertaining advice on structural matters.

TABLE OF CONTENTS

ACKNOWLEDGMENTS	Page iii
LIST OF TABLES.	vi
LIST OF ILLUSTRATIONS	viii
SUMMARY	ix
Chapter	
I. HISTORICAL INTRODUCTION.	1
Statement of Problem	
Monolayer Adsorption	
Multimolecular Adsorption	
II. EQUIPMENT AND PROCEDURE.	10
Vacuum System	
Pressure Measurement	
Constant Volume System	
Dosage Measurement	
The Adsorption Cell	
The Cryostat	
Sample Size and Treatment	
Materials	
Thermal Transpiration	
III. METHOD OF EVALUATING RESULTS	21
Adsorptive Potential	
Heterogeneity	
Isosteric Heat and Enthalpy of Adsorption	
Entropy Considerations	
Monolayer Capacity	
IV. EXPERIMENTAL RESULTS	33
V. DISCUSSION OF RESULTS.	39
Krypton on Boron Nitride	
Krypton on Graphite	
Recommendations for Further Study	

TABLE OF CONTENTS (Concluded)

	Page
APPENDICES.	47
A. EXPERIMENTAL DATA.	48
B. ISOSTERIC HEAT COMPUTATIONS AND ERROR ANALYSIS	54
C. SIGNIFICANT STRUCTURE THEORY COMPUTATIONS AND ERROR ANALYSIS	60
BIBLIOGRAPHY.	67

LIST OF TABLES

Table		Page
1.	Molecular Properties and Parameters for the Physical Adsorption of Krypton on Boron Nitride and Graphite. . .	41
2.	BET Plot Data Points	42
3.	Molar Integral Entropies of Adsorption for Krypton on Boron Nitride	44
4.	Multilayer Data for the Physical Adsorption of Krypton on Boron Nitride at 76.92 °K	49
5.	Multilayer Data for the Physical Adsorption of Krypton on Boron Nitride at 74.17 °K	50
6.	Multilayer Data for the Physical Adsorption of Krypton on Boron Nitride at 71.44 °K	51
7.	Monolayer Data for the Physical Adsorption of Krypton on Boron Nitride	52
8.	Monolayer Data for the Physical Adsorption of Krypton on Graphite.	53
9.	Monolayer Isosteric Heats of Adsorption for the Krypton-Boron Nitride System at 75.10 °K	58
10.	Multilayer Isosteric Heats of Adsorption for the Krypton-Boron Nitride System at 76.92 °K	59
11.	Significant Structure Theory Computations for the Krypton-Boron Nitride System at Various Temperatures $U_o = 2656 \text{ cal/mole}$, $\epsilon'/k = 118 \text{ °K}$, $\nu_o = 1.00 \times 10^{12} \text{ sec}^{-1}$, $A_o = 19.5 \text{ Å}^2/\text{molecule}$	62
12.	Significant Structure Theory Computations for the Krypton-Boron Nitride System at Various Temperatures $U_o = 2625 \text{ cal/mole}$, $\epsilon'/k = 118 \text{ °K}$, $\nu_o = 1.00 \times 10^{12} \text{ sec}^{-1}$, $A_o = 19.5 \text{ Å}^2/\text{molecule}$	63

LIST OF TABLES (Concluded)

Table		Page
13.	Significant Structure Theory Computations for the Krypton-Boron Nitride System at Various Temperatures $U_0 = 3000 \text{ cal/mole}$, $\epsilon'/k = 118 \text{ }^\circ\text{K}$, $\nu_0 = 1.00 \times 10^{12} \text{ sec}^{-1}$, $A_m^0 = 19.5 \text{ } \overset{\circ}{\text{A}}^2/\text{molecule}$	64
14.	Significant Structure Theory Computations for the Krypton-Boron Nitride System at Various Temperatures Assigning an Adsorptive Potential of 2625 cal/mole to Eighty Percent of the Surface and 3000 cal/mole to the Remaining Twenty Percent $\epsilon'/k = 118 \text{ }^\circ\text{K}$, $\nu_0 = 1.00 \times 10^{12} \text{ sec}^{-1}$, $A_m^0 = 19.5 \text{ } \overset{\circ}{\text{A}}^2/\text{molecule}$	65
15.	Significant Structure Theory Computations for the Krypton-Graphite System at Various Temperatures $U_0 = 2825 \text{ cal/mole}$, $\epsilon'/k = 118 \text{ }^\circ\text{K}$, $\nu_0 = 1.00 \times 10^{12} \text{ sec}^{-1}$, $A_m^0 = 19.5 \text{ } \overset{\circ}{\text{A}}^2/\text{molecule}$	66

LIST OF ILLUSTRATIONS

Figure		Page
1.	Schematic Diagram of Dosage System	14
2.	Schematic Diagram of Adsorption Cell	16
3.	Schematic Diagram of Cryostat.	17
4.	The Physical Adsorption of Krypton on Boron Nitride at 71.44 °K.	34
5.	The Physical Adsorption of Krypton on Boron Nitride at 74.17 °K.	35
6.	The Physical Adsorption of Krypton on Boron Nitride at 76.92 °K.	36
7.	The Physical Adsorption of Krypton on Boron Nitride - Significant Structure Theory Fit to Experimental Data. .	37
8.	The Physical Adsorption of Krypton on Boron Nitride - Two Part Significant Structure Theory Fit to Experi- mental Data.	38
9.	Isosteric Heats of Adsorption of Krypton on Boron Nitride at 75.10 °K.	43
10.	The Physical Adsorption of Krypton on Graphite - Significant Structure Theory Fit to Experimental Data. .	46

SUMMARY

A series of low pressure isotherms in the temperature range 71.5°K to 77.0°K were measured for both the krypton-boron nitride and the krypton-graphite, P33(2700°), systems.

The krypton-boron nitride multilayer region was found to be remarkably similar to that of the argon-boron nitride system as measured by Pierotti.²² From the sub-monolayer data, it was determined that the surface consisted of two distinct types of adsorption sites. The theoretical analysis of the experimental results, using a significant structure theory of physical adsorption, yielded that eighty percent of the surface was made of isotactic patches with an adsorptive potential of 2625 cal/mole \pm 6 cal/mole. An adsorptive potential of 3000 cal/mole \pm 6 cal/mole was found for the remaining twenty percent of the surface. The lateral interaction parameter, ϵ'/k , and the characteristic frequency for the vibration of the adsorbate normal to the surface, ν_0 , were found to be 118°K \pm 1°K and $1.00 \times 10^{12} \text{ sec}^{-1} \pm 0.02 \times 10^{12} \text{ sec}^{-1}$, respectively.

Entropy considerations showed the system to be mobile. The two-dimensional critical temperature as determined from the significant structure theory was 70.75°K \pm 0.60°K. The isosteric heats at 75.10°K were of the usual form with peaks in the neighborhood of unit coverage and with a limiting value of 2720 cal/mole \pm 100 cal/mole at zero coverage. A value of 4.61 cc(STP)/gm \pm 0.06 cc(STP)/gm was assigned to V_m through the use of a BET plot.

The krypton-graphite isotherms were also fitted with the signifi-

cant structure theory. A value of $2825 \text{ cal/mole} \pm 6 \text{ cal/mole}$ was determined for the adsorptive potential and $70.75^\circ\text{K} \pm 0.60^\circ\text{K}$ for the two-dimensional critical temperature. The fact that ν_0 and ϵ'/k were found to be the same as in the krypton-boron nitride was not expected but was certainly acceptable within the experimental error.

CHAPTER I

INTRODUCTION

Statement of Problem

In 1950 J. H. De Boer¹ pointed out that calculations dealing with adsorption forces could only give the correct order of the magnitude since

1. we do not know the real structure of the surface;
2. we do not know, really, the repulsion forces, checking the attracting forces at short distance;
3. we do not know the real distance of the adsorbed atom from the surface.

However, by limiting oneself to the case of adsorption on a nearly homogeneous surface, one can minimize these uncertainties.

The purpose of this work is to investigate one such ideal case, The adsorption of krypton on boron nitride. The next logical step would be, of course, to extend the model to explain the phenomena encountered on the surface of the more heterogeneous solids.

The ensuing discussion shall treat the development of models based on mobile and localized monolayers with emphasis on the former. Finally, a logical extension of the mobile monolayer model shall be made to include multi-layer adsorption.

As mentioned briefly, the complexities of physical adsorption are greatly reduced when working with a homogeneous surface. Graphite and boron nitride are examples of adsorbents with such surfaces. A number of workers²⁻⁷ have investigated the interaction of the rare gases with these

adsorbents and have observed clear, step-like isotherms which would seem to indicate surface homogeneity.

One such system, the boron nitride-krypton system, has been partially investigated in the monolayer region by Pultz² and Cripps.³ However, there has been no extensive determination of the thermodynamic properties of this system in either the monolayer or multilayer regions. Such is the primary objective of this work.

The phenomenon of two-dimensional condensation has been reported by several workers. Ross and Winkler⁴ have reported the two-dimensional condensation of krypton on graphite at 77.8°K, whereas Clark⁵ observed no such phenomena at temperatures greater than 70.2°K. In addition, Pierotti⁶ has determined krypton-graphite isotherms at 74.9°K and Singleton and Halsey⁷ at 77°K, and neither observed two-dimensional condensation at these temperatures. Ross and Pultz² and Cripps³ have also reported such condensation for the krypton-boron nitride system at 77.8°K. However, the uncertainty as to the true value of the two-dimensional critical temperature for the krypton-graphite system would seem to warrant a redetermination of this property for both krypton-graphite and krypton-boron nitride systems.

Monolayer Adsorption

Background

The physical adsorption of a gas by a solid surface is a phenomenon which takes place to some extent at all pressures and the adsorbed film may be thought of as a separate two-dimensional phase. The degree of adsorption at any given temperature and equilibrium pressure depends upon

the interaction of the gas with the solid, the lateral interaction of the adsorbed molecules, the fundamental frequency of vibration of the adsorbed molecule normal to the surface, the area per molecule at monolayer coverage, and finally the degree of homogeneity of the surface.

One means of observing a two-dimensional phase is through the use of a film balance introduced by Langmuir⁸ in 1917 to measure the spreading pressures of insoluble monolayers on a liquid surface. The resulting two-dimensional equation of state found for many systems is

$$\Pi\sigma = kT$$

where Π is the spreading pressure in dynes per square centimeter, σ is the surface area per molecule, k is the Boltzmann constant, and T is the absolute temperature. It appears that for these systems the adsorbed phase behaves as though it were a two-dimensional ideal gas. It is, therefore, not unreasonable to expect that a two-dimensional van der Waals type equation might better represent the state of non-ideal two-dimensional behavior.

If, however, we are working with the adsorption of a gas on a solid surface, the equilibrium pressure, P , and not Π is the measurable quantity. Fortunately, knowledge of the specific surface area, A , permits any equation of state to be converted to the corresponding isotherm equation through the use of the Gibbs adsorption isotherm,⁹

$$\Pi = RT/(22,400A) \int_0^P V d \ln P$$

where A is in the units cm^2/gm and R is in the units $\frac{\text{dyne cm}^2}{\text{gm}^2 \text{K}}$ or in another form

$$\Pi = kT/\sigma_o \int_0^P \theta d \ln P$$

σ_o is the area per molecule at monolayer coverage and θ is the fraction of the surface covered such that

$$\theta = \sigma_o/\sigma$$

The application of the Gibbs equation to the equation of state $\Pi\sigma = kT$ generates the isotherm equation $p = K\theta$ which is the Henry's law equation for physical adsorption. Similarly, any two-dimensional equation of state may be transformed into its corresponding isotherm equation.

Localized Adsorption

One of the first completely theoretical treatments of the adsorption isotherm was given by Langmuir.¹⁰ In his choice of models, Langmuir hypothesizes that the rate of adsorption, R_a , is proportional to the pressure of the gas above the solid and to the fraction of the surface not covered, $1-\theta$. The rate of desorption, R_d , is proportional to the fraction of the surface covered, θ .

$$R_a = K_1 P(1 - \theta)$$

$$R_d = K_2 \theta$$

at equilibrium

$$R_a = R_d$$

$$P = K\theta/(1 - \theta)$$

However, in deriving the above equation, Langmuir assumes that the adsorptive potential is uniform throughout, and the adsorbate-adsorbate interaction is negligible. This is rarely the case. However, since in general these two effects act in opposite directions, they tend to cancel out, thus explaining the success of the Langmuir equation in describing many systems. Langmuir's remaining assumptions are that the gas phase behaves ideally, the amount adsorbed is confined to a mono-molecular layer and the adsorbed molecules are localized. These assumptions are true for many, but certainly not all systems.

The equation of state most frequently used to describe localized adsorption is the Fowler-Guggenheim equation,¹¹

$$\Pi\sigma = kT \sigma/\beta \ln [\sigma/(\sigma - \beta)] - (cw/2)(\beta/\sigma)$$

where w is defined as the interaction energy per pair of nearest neighbors at their equilibrium distance of separation, and c is related to the coordination number of the lattice. The product cw differs for each adsorbate-adsorbent system. α and β are the two-dimensional van der Waals constants corresponding to the three-dimensional case, and σ is the surface area per molecule.

As opposed to the Langmuir model, the Fowler-Guggenheim model includes lateral interaction and does not assume that the gas phase behaves ideally. Upon transformation by the Gibbs equation, the corresponding isotherm equation¹² is found to be

$$P = K\theta/(1 - \theta) \exp (- cw\theta/kT)$$

where K is an integration constant dependent upon the adsorptive potential, U_0 , and T , but independent of θ .¹³

Mobile Adsorption

One of the most useful equations of state used to describe mobile adsorption is the two-dimensional van der Waals equation,¹⁴

$$(\Pi + \alpha/\sigma^2)(\sigma - \beta) = kT.$$

α , β , and σ are defined in the same manner as in the Fowler-Guggenheim equation and K is again an integration constant dependent upon the adsorptive potential and T , but independent of θ . Upon transformation, the corresponding isotherm equation is found to be

$$P = K\theta/(1 - \theta) \exp [\theta/(1 - \theta) - 2\alpha\theta/(kT\beta)].$$

More recently, McAlpin and Pierotti^{15,16} have undertaken a statistical development for monolayer adsorption on a homogeneous surface based upon the significant structure theory of liquids.¹⁷ This work has proven to be of great value in describing the physical adsorption of many of the

inert gases on homogeneous surfaces. The discussion of this work may be found in Chapter III.

Multimolecular Adsorption

In 1938, Brunauer, Emmett, and Teller¹⁸ generalized the Langmuir theory to include the case of multimolecular adsorption to an infinite number of layers. The equation they derived is

$$\theta = cx / [(1 - x)(1 - x + cx)]$$

where $x = P/P_0$, and P_0 represents the saturation vapor pressure of the adsorbate. Now

$$c = (a/b) g \exp [(E_1 - E_L)/RT]$$

where E_1 is the heat of adsorption of the first layer, E_L is the heat of liquification, and g , a , and b are also constants.

If the thickness of the adsorbed phase is finite, then one obtains the equation

$$\theta = \frac{cx}{1 - x} \left\{ \frac{1 - (n + 1)x^n + nx^{n+1}}{1 + (c - 1)x - cx^{n+1}} \right\}$$

where n is the maximum number of layers.

Unfortunately, as with the Langmuir theory, the BET model assumed localized adsorption in the first layer, and no lateral interaction in

any of the layers.

Hill,¹⁹ through a statistical mechanical treatment, derived isotherm equations which included lateral interaction. Subsequently, Champion and Halsey²⁰ modified the Hill equations to take into account the energy transmitted from the adsorbent to the n^{th} layer. They found that

$$P/P_0 = [(\theta_n - \theta_{n+1})/(\theta_{n-1} - \theta_n)] \exp [- E_n/kT + (w/kT) \\ \times (- 2\theta_n + 1)]$$

where θ_n is the coverage in the n^{th} layer, w is the lateral interaction energy, and

$$E_n = E_1/n^3$$

which is the inverse cube law for energy decay.

Champion and Halsey next reasoned that if the lattice structure of the adsorbate was not compatible with that of the adsorbent, the adsorbate molecules might not assume the optimum configuration for interaction. Therefore, w would be reduced and the isotherm would proceed without steps.

The equation modified to account for this feature is

$$P/P_0 = [(\theta_n - \theta_{n+1})/(\theta_{n-1} - \theta_n)] \exp [- E_n/kT + (w/kT) \\ \times (- 2g_n\theta_n + 1)]$$

where the parameter g_n varies from zero in the first layer to unity where n is large.

Finally, Singleton and Halsey²¹ pointed out that if g_n was taken as a constant for all layers, and $\theta_n = 1/2$, $\theta_{n-1} = 1$ and $\theta_{n+1} = 0$ that

$$\ln(P/P_0) = - E_1/(n^3 kT) + (w/kT)(1 - g)$$

which is an equation for the pressure at the n^{th} step.

CHAPTER II

EQUIPMENT AND PROCEDURE

The apparatus is a modification of the adsorption apparatus designed and built by Pierotti.²² The structure consists primarily of six inter-related parts all of which together constitute a form of the high vacuum adsorption apparatus.

Vacuum System

Main Pumping System

The main pumping system consists of a two-stage mercury diffusion pump with a liquid nitrogen trap connected in series with a mechanical forepump. Vacuums in the neighborhood of 10^{-6} to 10^{-7} millimeters of mercury may be obtained with such a system.

Auxiliary Pumping System

The auxiliary system serves to control the mercury levels in the McLeod gauge, gas burette, constant volume system, and Toepler pump. A small mechanical pump adapts well to this purpose.

Pressure Measurement

The measurement of equilibrium pressure, along with temperature control, is possibly the most crucial step in the determination of an adsorption isotherm. Since this experiment necessitates pressure measurements in the range of several microns up to two millimeters of mercury, a thermistor pressure gauge was chosen. At higher equilibrium pressures,

the constant volume manometer, to be described in the determination of dead space, may be used.

A thermistor was chosen for several reasons. Foremost, of course, is its applicability to low pressure measurement. However, also of considerable importance is its small constant volume, and the ease with which the equilibrium process may be followed.

The Thermistor Pressure Gauge, Model MIC-401 of the Numec Instruments and Controls Corporation, was kindly supplied by Dr. Clyde Orr and Mr. Warren Hendricks both of the School of Chemical Engineering of the Georgia Institute of Technology.

The thermistor, a semi-conductor, is contained in a constant temperature bath and is heated by means of a small electric current, the magnitude of which is determined by the temperature of the thermistor. Gas contact with the thermistor brings about the conduction of heat away from the thermistor. The greater the pressure of the gas, the more rapid is the conduction of heat and the associated rise in resistance. Consequently, through the use of a Wheatstone bridge, in which the thermistor is one of the elements, pressure can be directly related to the resistance of the thermistor.

To obtain more precise readings at pressures in the range zero to twenty microns, a Graphicorder-10, manufactured by the Dynatron Instruments Corporation, is placed across the gauge output. The recorder permits pressure measurements with a precision of approximately 0.1 microns in the above pressure range. At greater pressures, the precision of the reading is approximately one-half of the smallest gauge unit or 0.25 microns at twenty microns total pressure and varies up to five microns at

1.5 millimeters total pressure. At pressures greater than 1.5 millimeters, the thermistor is too insensitive to obtain meaningful readings.

It is found that the instrumental design of the ambient temperature control for the thermistor gauge is such that the zero of the instrument fluctuates the order of one micron with changing room temperature. To minimize this zero drift, a small heater coil is placed around the thermistor casing and the outside of the coil is maintained at constant temperature.

Such precautions are not taken in the initial runs of the multilayer isotherms on boron nitride; therefore, the monolayer isosteric heats are evaluated from the set of isotherms measured exclusively in the sub-monolayer region. In this instance, both the heater coil and recorder are employed to obtain more significant readings.

The absolute value of the pressure at any given thermistor reading is measured directly by means of a high precision McLeod gauge. The calibration can be easily reproduced over a period of time as long as the thermistor is not exposed to mercury. Therefore, traps which are kept at dry ice-acetone temperature are placed between all mercury sources and the sample tube.

After the calibration, the McLeod gauge is cut off from the thermistor system. It should also be noted that the thermistor gauge can be calibrated with the sample tube open to the thermistor since krypton is not appreciably adsorbed on boron nitride at room temperature.

Constant Volume System

A conventional constant volume apparatus is used to determine the

dead space of the system. The constant volume system, in conjunction with a cathetometer graduated to 0.01 millimeters may be used to measure pressures out of the range of the thermistor gauge.

The gas chosen for the determination of dead space is helium, since it is not appreciably adsorbed at the isotherm sample temperature. Both the volumes at room and sample temperatures are determined to within 0.1 cc. This gives a maximum percentage error of approximately 2.5×10^{-4} percent due to dead space determination at a pressure of 2 mm in the highest temperature isotherm (77°K).

The volume of krypton remaining in the gas phase is found to be negligible compared to the volume adsorbed in the multilayer isotherms due to the large sample size. The same is found to be true in the small sample runs since the sub-monolayer pressures were extremely small.

Dosage Measurement

A previously calibrated gas burette is used in conjunction with a mercury U-tube manometer and a cathetometer graduated to 0.01 millimeters to measure the size of the dose to within three micro liters. By varying the volume in the Toepler pump the approximate size of the dose desired can be controlled, see Figure 1.

The Adsorption Cell

The adsorption cell is similar in design to that of Singleton and Halsey.²³ The cell itself is suspended by its leads in a vacuum jacket which can be filled with an exchange gas such as helium. In order to reduce the effect of thermal transpiration, glass tubing of five millimeters inside diameter is used between the sample tube and a point just

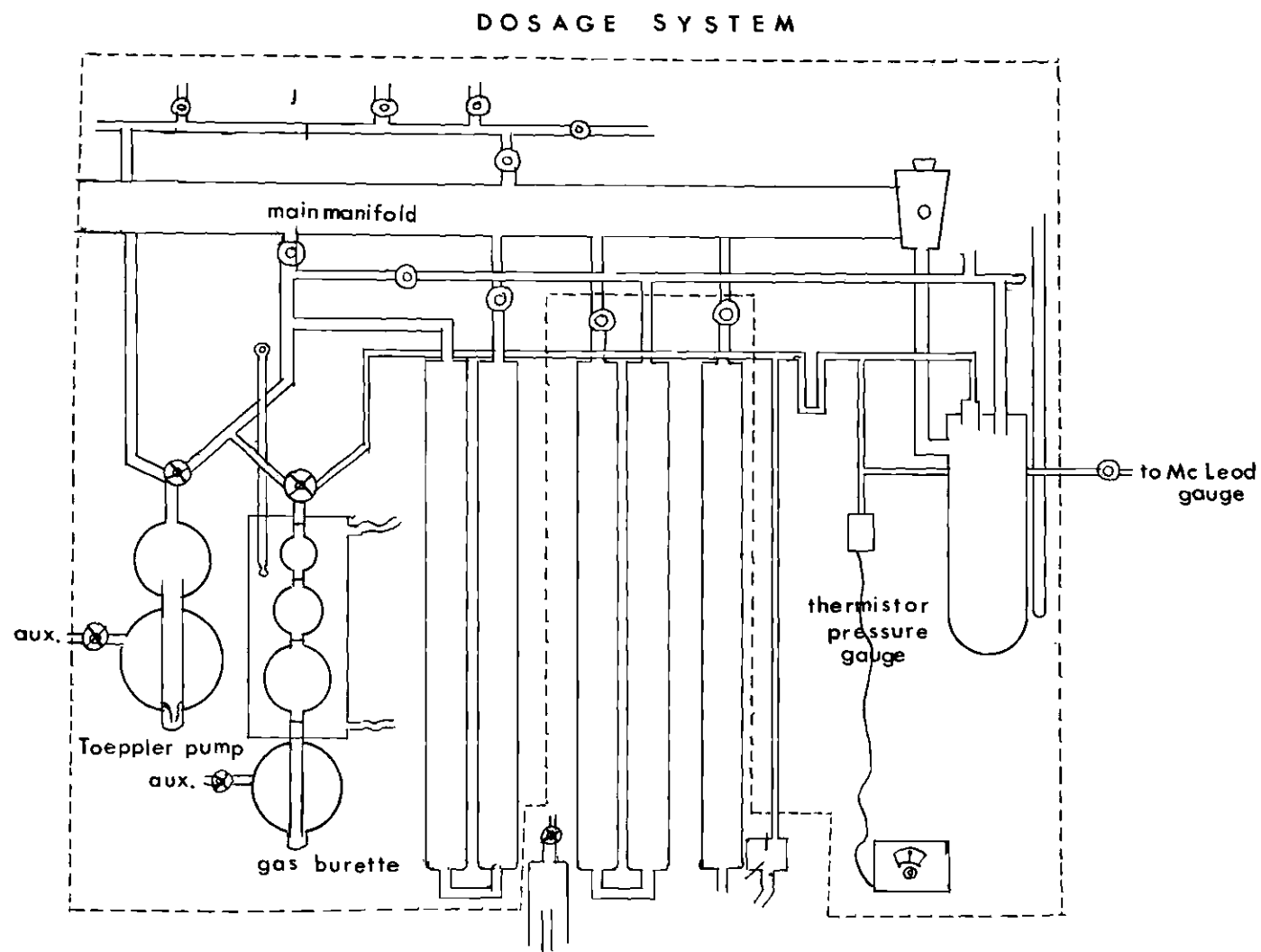


Figure 1. Schematic Diagram of Dosage System

above the glass vacuum jacket. Small bore capillary tubing of one millimeter inside diameter is used throughout the remainder of the adsorption system in order to minimize the dead space, see Figure 2.

The Cryostat

The cryostat is similar in design to that of Lytle and Stoner.²⁴ To obtain the desired temperature, helium may be bubbled through liquid nitrogen in the range 70°K to 77°K and liquid oxygen in the range of 77°K to 90°K. Since helium is only very slightly soluble in either of these liquids, some of the liquid evaporates into the helium bubbles as it passes through, thereby lowering the temperature. Greater cooling efficiency is achieved by using the exhaust gases to pre-cool the helium. An argon vapor pressure thermometer is used to control the cryostat temperature at any of several preselected values. The system is diagrammed in Figure 3.

The actual isotherm temperature is measured by a separate argon thermometer which is connected by glass tubing to a thermo-well located in the sample tube. Such a design permits temperature control to within 0.04°K.

Sample Size and Treatment

The boron nitride sample is initially outgassed for twelve hours at 400°C and then for two days at 500°C. Between isotherm runs, the sample is outgassed at 500°C for twelve hours.

The graphite sample is initially outgassed at 300°C for several hours and then at 425°C for two days. The sample is outgassed at 400°C between isotherm runs for a period of twelve hours.

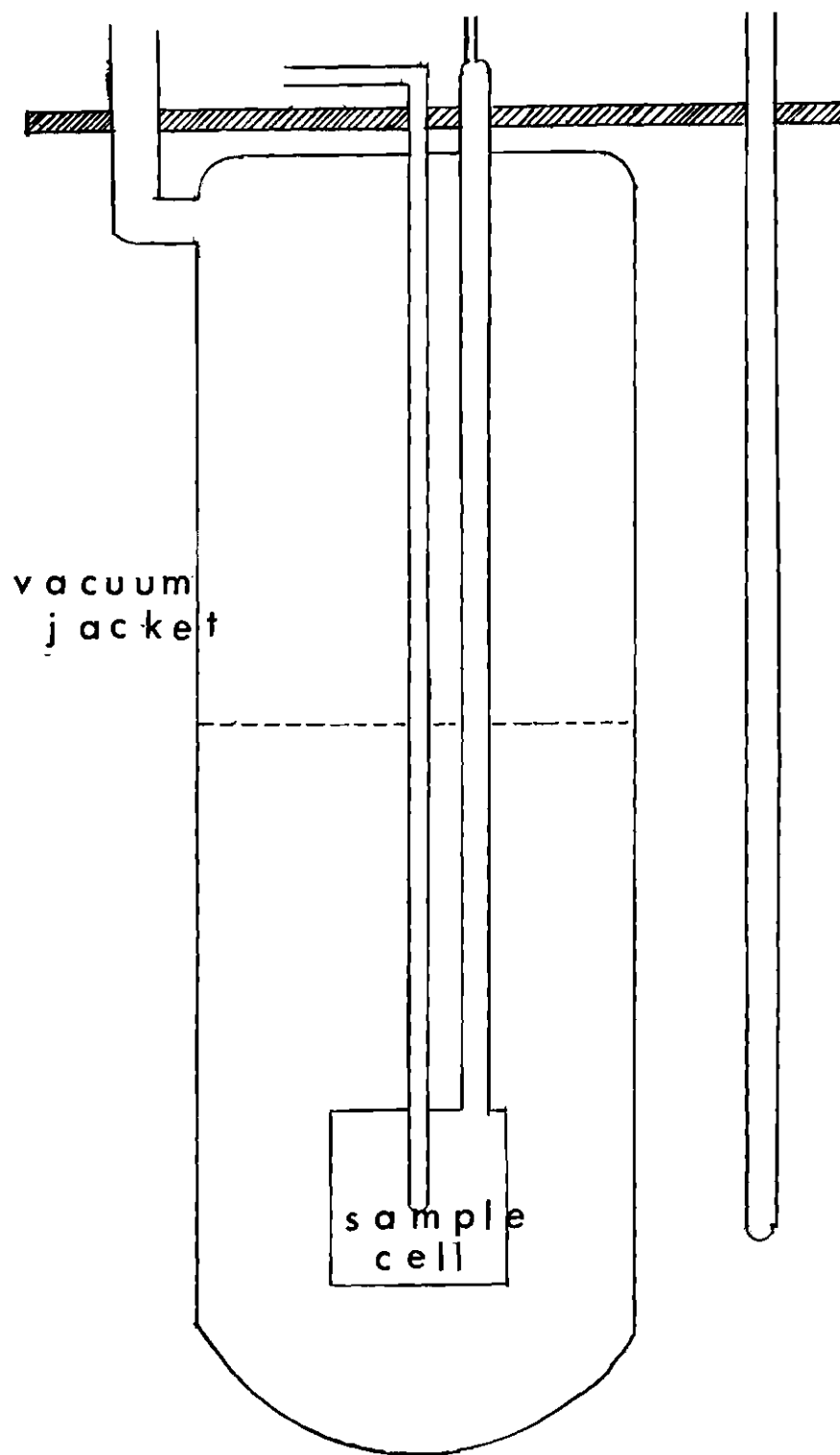


Figure 2. Schematic Diagram of Adsorption Cell

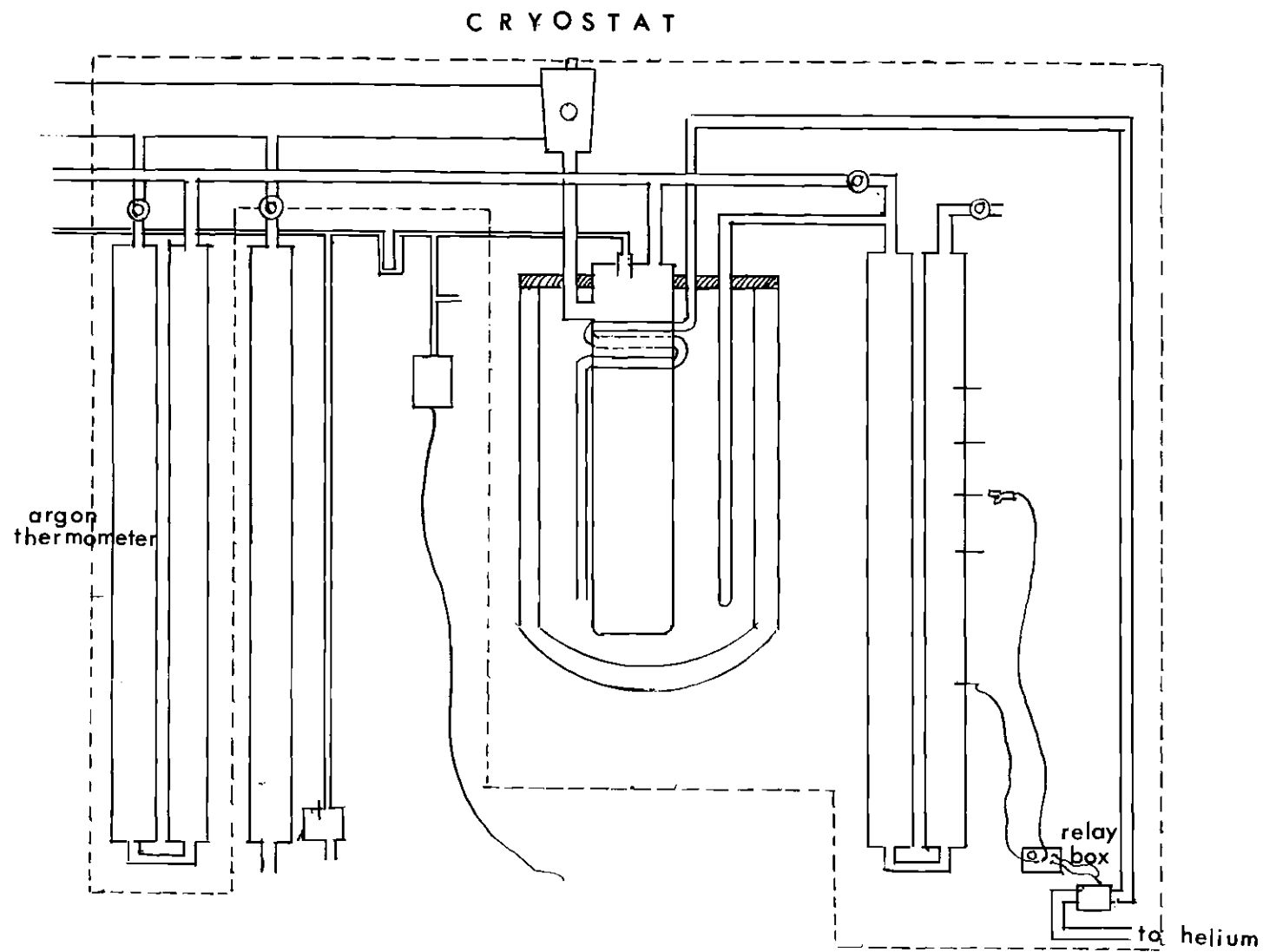


Figure 3. Schematic Diagram of Cryostat

At first, a one gram boron nitride sample is used. However, it is found that such a large sample requires in some instances upwards of three hours for equilibrium per point. This effect is more prevalent in the lower temperature isotherms. One possible explanation is that the krypton is at first adsorbed in multilayers in the upper portion of the sample and then has to desorb and diffuse to the lower portion of the sample before equilibrium can be obtained.

To permit rapid equilibrium, a new sample of about 0.1 gram of boron nitride is spread over the bottom of a flat bottomed sample tube as suggested by Clark.⁵ The new equilibrium time is found to be between twenty and thirty minutes. A similar container is used to contain the graphite sample. The sample weighs about 0.25 gram.

Materials

Assayed reagent, spectroscopically pure krypton in pyrex flasks obtained from Air Reduction Sales, Inc. is used without further purification.

The boron nitride powder, 325 mesh, is obtained from the Research and Development Division of the Carborundum Company. Spectrographic analysis shows it to be greater than 99.92 percent pure. X-ray diffraction showed it to be highly crystalline, having a crystal structure similar to that of graphite.

The graphite obtained from Dr. Carl Prenzlow is prepared by Dr. W. Smith of Godfrey Cabot Company and designated Sterling FT (2700°). It is the same as P-33 (2700°).

Thermal Transpiration

If two parts of a system are at different temperatures, gas will diffuse from the lower to the higher temperature region. When the pressure difference is sufficient to balance this transpiration, a steady state is obtained. The effect is greatest when the mean free path of the gas molecule is much greater than the inside diameter of the tube through which the gas is passing. Thus, by increasing the diameter of the tube, or decreasing the mean free path length by increasing the pressure, the effect is minimized.

Weber²⁵ developed an equation for the thermal transpiration of a gas along a closed cylindrical tube

$$dP/dT = P/2T (1/(\alpha y^2 + \beta y + u)) \quad y = d/\lambda$$

where P is the pressure, T is the temperature, d is the diameter, and λ is the mean free path length of the gas molecules.

$$\alpha = \pi/128$$

$$\beta = \pi/12$$

$$u = (1 + gy)/(1 + hy)$$

$$g - h + \beta = 1 \text{ or } 3/4$$

$$g/h \approx 1.25$$

Miller²⁶ has suggested the following approximate solution.

$$(dP/dT)(2T/P) \cong \Delta P/\Delta T \cong 2T/P \cong \frac{1 - (P_1/P_2)}{1 - (T_1/T_2)^{\frac{1}{2}}} = X$$

$$X = 1/(\alpha y^2 + \beta y + u) \quad T_2 > T_1$$

The value of y is calculated using the kinetic theory of gases to determine the mean free path as a function of T and P . It is found that

$$y = (P_2 d \sigma^2 / 2.33T) \times 10^3$$

$$T = (T_1 + T_2)/2$$

$$\sigma_T^2 = \sigma_\infty^2 (1 + C/T)$$

C is a constant for a given gas and σ_∞ is the limiting molecular hard sphere diameter at high temperature. Values of C and σ_∞ for many gases are tabulated in Landolt-Bornstein.²⁷

On the basis of work done by Rosenberg, Miller has calculated $\alpha = 0.0322$ and $\beta = 0.262$ for krypton. The resulting equation is

$$X = (0.0322y^2 + 0.262y + (1 + 2.5y)/(1 + 2y))^{-1}$$

The above equation is used in this experiment for the purpose of correcting measured equilibrium pressures.

CHAPTER III

METHOD OF EVALUATING RESULTS

Adsorptive Potential

In this work, the significant structure equation of McAlpin and Pierotti^{15,16} is used to evaluate the experimental value of U_o from monolayer isotherm data. Their model considers three degrees of freedom for the adsorbed molecule; a two-dimensional gas-like degree of freedom associated with translation on the surface, a solid-like degree of freedom associated with restraint to a lattice site by nearest neighbors, and a configurational degeneracy associated with nearest neighbor vacancies. The contribution of each significant structure varies with the fractional coverage.

The resulting isotherm equation is

$$\begin{aligned} \ln P = & - u_{\text{gas}}^o/kT + U_o/RT(2\theta - 1) - \ln(C/\theta) \\ & - 2\theta \ln \left\{ (B\theta/C)(1 + Z(1 - \theta)/\theta) \right\} \\ & + 1 + (Z - 1)\theta^2/[Z - (Z - 1)\theta] \end{aligned} \quad (1)$$

where u_{gas}^o is the standard chemical potential of the gas phase in equilibrium with the adsorbed phase, and

Z is the number of nearest neighbors on the surface.

$$B = D(2\pi mkT/h^2) a_f \exp (W/RT) \quad (2)$$

where

$$a_f = \pi a^2 \int_0^{\frac{1}{4}} \left\{ \exp (6\epsilon'/kT)(2m_s(y) - l_s(y)) \right\} dy \quad (3)$$

where

a is the nearest neighbor distance in the two-dimensional solid
and is taken as the equilibrium distance in the bulk adsorbate
 y is a reduced distance parameter and is given by

$$y = a^2/r^2 \quad (4)$$

where

r is the nearest neighbor distance of the adsorbate on the surface
at a given coverage

$m_s(y)$ and $l_s(y)$ for the inert gases are given by Devonshire²⁸ where

$$m_s(y) = (1 + 4y + y^2)(1 - y)^{-5} - 1 \quad (5)$$

and

$$l_s(y) = (1 + y)(1 + 24y + 76y^2 + 24y^3 + y^4)(1 - y)^{-11} - 1 \quad (6)$$

ϵ' is the Lennard-Jones potential parameter corrected for the third-order dispersion effect.

$$C = D(2\pi mkT/h^2) A_m^0 e \quad (7)$$

where A_m^0 is the area per molecule at monolayer coverage.

$$D = \frac{\exp(-h\nu_o/2kT)}{1 - \exp(-h\nu_o/kT)} \quad (8)$$

where ν_o is the fundamental frequency of vibration of the adsorbed molecule normal to the surface.

Heterogeneity

The isotherm equations in Chapter I are all based on adsorption on a homogeneous surface, that is the adsorptive potential, U_o , is the same at all points on the surface. This, of course, is an idealization which is seldom, if ever, obtained.

The following is the treatment of heterogeneity given by Ross and Oliver.²⁹ The surface is considered to consist of an infinitesimal number of energy patches which adsorb independently of each other. The distribution of energy among these patches is considered to be Gaussian. The greater the homogeneity of the surface, the more peaked will be the distribution.

The isotherm itself can be obtained by treating each patch separately and summing up over the patches

$$K_i = A^o e^{-U_{oi}/RT}$$

where U_{oi} is the adsorptive potential of the i^{th} patch.

The effective contribution of the i^{th} patch coverage $\Phi(P, U_{oi})$ to the total coverage, $\theta(P)$, is given by

$$d\theta(P) = \Phi(P, U_{oi}) \rho(U_{oi}) dU_{oi}$$

where $\rho(U_{oi})$ is the density of sites with adsorptive potential, U_{oi} .

Thus by summing over the entire range of adsorptive potentials, a value for $\Phi(P)$ may be determined.

The resultant equation is given by

$$\theta(P) = \int_0^{\infty} \Phi(P, U_{oi}) \rho(U_{oi}) dU_{oi}$$

For a Gaussian distribution of adsorptive potentials

$$\rho(U_{oi}) = 1/N e^{-\gamma(U_{oi} - U_o')^2}$$

where U_o' is the average adsorptive potential of the distribution

N is a normalization factor

γ is a measure of the breadth of the distribution and is inversely proportional to the degree of heterogeneity.

The normalization factor is given by

$$N = \int_0^{\infty} e^{-\gamma(U_{oi} - U_o')^2} dU_{oi}$$

For a non-Gaussian distribution of adsorptive potentials, the sum may be taken in the following manner.

$$\theta(P) = \rho(U_{o1})\theta(P, U_{o1}) + \rho(U_{o2})\theta(P, U_{o2}) + \dots$$

$$\dots + [1 - \sum_{i=1}^{n-1} \rho(U_{oi})]\theta(P, U_{on})$$

In this case

$$\rho(U_{oi}) = (1/N)x_i$$

where N is the total number of adsorptive sites and x_i is the number of sites of adsorptive potential U_{oi} .

Isosteric Heats and Enthalpy of Adsorption

The isosteric heats of adsorption are calculated by means of the Clausius-Clapeyron equation

$$q_{st}/RT^2 = (\partial \ln P / \partial T)_{\theta}$$

where q_{st} is the isosteric heat.

Now in general

$$\frac{\partial q_{st}}{\partial T} = \Delta C_p \quad (10)$$

and

$$q_{st} = \int_0^T \Delta C_p dT + q_{st}^0 \quad (11)$$

where q_{st}^0 corresponds to the isosteric heat at zero degrees absolute.

Therefore

$$\ln P = \int \left(\frac{\Delta C_p dT}{RT^2} + \frac{q_{st}^0}{RT^2} \right) dT \quad (12)$$

integrating

$$\ln P = (\Delta C_p/R) \ln T - q_{st}^0/RT + B \quad (13)$$

where B is a constant of integration.

Minimization of the least square error function with respect to q_{st}^0 , C_p , and B yields the three following equations:

$$0 = \sum_{i=1}^n \ln P_i / T_i + q_{st}^0 / R \sum_{i=1}^n 1/T_i^2 - \Delta C_p / R \sum_{i=1}^n \ln T_i / T_i - B \sum_{i=1}^n 1/T_i \quad (14)$$

$$0 = \sum_{i=1}^n \ln P_i \ln T_i + q_{st}^0 / R \sum_{i=1}^n \ln T_i / T_i - \Delta C_p / R \sum_{i=1}^n (\ln T_i)^2 - B \sum_{i=1}^n \ln T_i \quad (15)$$

$$0 = \sum_{i=1}^n \ln P_i + q_{st}^0 / R \sum_{i=1}^n 1/T_i - \Delta C_p / R \sum_{i=1}^n \ln T_i - nB \quad (16)$$

where n is the number of different isotherms employed in the determination.

At any given temperature, T,

$$q_{st} = q_{st}^0 + \int_0^T \Delta C_p dT \quad (17)$$

The differential heat of adsorption, q_{diff} , can be shown to be

$$q_{\text{diff}} = q_{\text{st}} - RT \quad (18)$$

In this work, the following method of calculating, ΔH_a , the molar integral enthalpy of adsorption, is used as an intermediate step in determining the integral molar entropy change on adsorption, ΔS_a , based upon two reasonable alternate models. Ross and Oliver³⁰ have shown that for a two-dimensional van der Waals gas ΔH_a is given by the expression

$$\Delta H_a = - q_{\text{diff}} + RT[\theta/(1 - \theta)] \quad (19)$$

while for a localized system obeying Fowler-Guggenheim adsorption ΔH_a is given by

$$\Delta H_a = - q_{\text{diff}} - RT + (RT/\theta)\ln(1/1 - \theta) \quad (20)$$

Using equation (18) one obtains

$$\Delta H_a = - q_{\text{st}} + RT(1 + \theta/1 - \theta) \quad \text{van der Waals} \quad (21)$$

$$\Delta H_a = - q_{\text{st}} + (RT/\theta)\ln(1/1 - \theta) \quad \text{Fowler-Guggenheim} \quad (22)$$

The molar integral Gibbs free energy change of adsorption is given by

$$\Delta G_a = RT\ln(P/760) \quad (23)$$

where P is in millimeters of mercury and also by

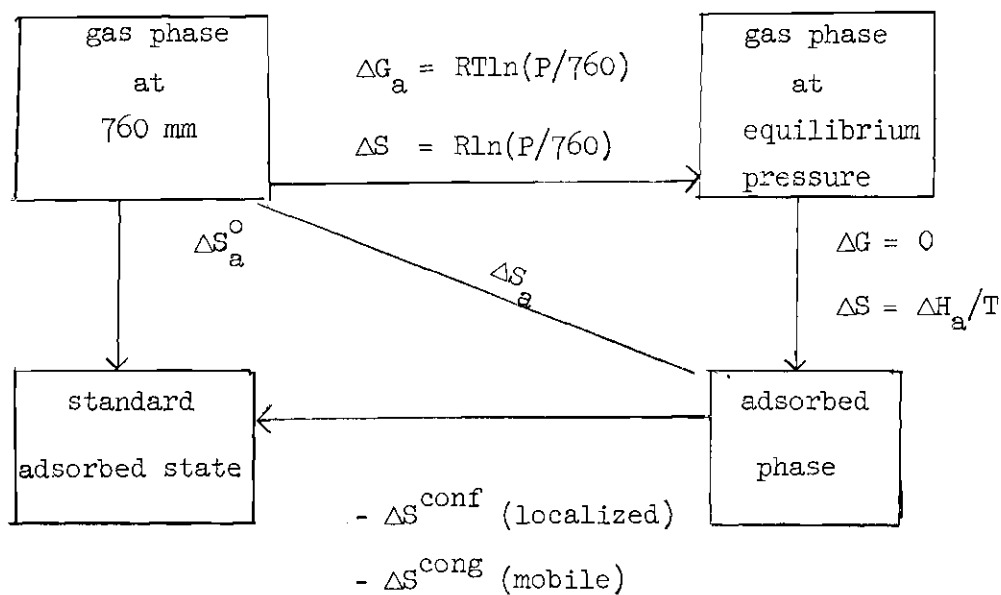
$$\Delta G_a = \Delta H_a - T \Delta S_a \quad (24)$$

Therefore, it is possible to obtain ΔS_a for each model from experimental measurements and the assumed alternate models since

$$\Delta S_a = \frac{\Delta H_a - \Delta G_a}{T} \quad (25)$$

Entropy Considerations

The determination of the standard integral entropy of adsorption, ΔS_a^0 , presents one method of determining whether the particular system is mobile or localized.



From the above cycle, it can be seen that

$$\Delta S_a^0 = \Delta H_a/T + R \ln(P/760) - \begin{cases} \Delta S^{\text{conf}}_{\text{localized}} \\ \Delta S^{\text{cong}}_{\text{mobile}} \end{cases} \quad (26)$$

In mobile adsorption, the standard state is often chosen as the coverage, θ_s , at which the intermolecular separation of the adsorbate molecules in the surface phase is the same as in the gas phase.³¹⁻³⁴

That is

$$\theta_s = \frac{\beta}{\sigma_s} = \frac{\beta}{4.08T} \quad (27)$$

where β is the two-dimensional van der Waals constant corresponding to b in the three-dimensional case, and σ_s is the area per molecule in the standard state of the adsorbed phase.

It can in fact be shown that for mobile adsorption the entropy of congregation³² is

$$\Delta S^{\text{cong}} = - R \ln \left\{ [\theta/(1 - \theta)] / [\theta_s/(1 - \theta_s)] \right\} \quad (28)$$

In the localized model, θ_s is determined by the spacing of the adsorption sites and not by the dimensions of the adsorbate molecules. It is usually taken as 0.5 and the corresponding entropy change from the standard state, S^{conf} , the entropy of configuration, accounts for the number of different ways of arranging the adsorbed molecules among the surface sites.³³

$$\Delta S^{\text{conf}} = - R[\ln\theta/\theta_s + (1 - \theta)/\theta \ln(1 - \theta) - (1 - \theta_s)/\theta_s \ln(1 - \theta_s)] \quad (29)$$

For the adsorption of krypton, the total entropy change would be the sum of the translational, ΔS_{tr} , and vibrational, ΔS_{vib} , entropy changes. The rotational change is zero since krypton has no rotational entropy in either the gaseous or adsorbed state. For the purpose of testing experimental results against mobile and localized models, one drops the vibrational entropy change since it is usually small in relation to the translational entropy change.

For the localized case,

$$\Delta S_a^{\circ} = - g^{\circ}_{\text{tr}} \quad (30)$$

where g°_{tr} is the translational entropy in the gaseous state and can be approximated by means of the Sackur-Tetrode equation for the standard molar entropy of an ideal gas.

$$g^{\circ}_{\text{tr}} = R \ln(M^{3/2} T^{5/2}) - 2.30 \quad (31)$$

where g°_{tr} is expressed in cal/mole °K.

For the mobile case

$$\Delta S_a^{\circ} = - g^{\circ}_{\text{tr}} + a^{\circ}_{\text{tr}} \quad (32)$$

where $S_{a\text{tr}}^{\circ}$ as derived by de Boer and Kruyer³⁴ is the translational entropy based on a two-dimensional ideal gas at a standard state spreading pressure of 0.338 dynes/cm.

$$S_{a\text{tr}}^{\circ} = 2/3 S_{g\text{tr}}^{\circ} + 1.52 \log T - 3.04 \quad (33)$$

where $S_{a\text{tr}}^{\circ}$ is expressed in cal/mole °K.

Monolayer Capacity

Previously, a number of references have been made to the quantity θ , the fraction of the surface covered. Unfortunately, in order to determine θ the volume of the monolayer, V_m , a quantity of some uncertainty, must first be determined.

The two most popular methods of evaluation of V_m are by means of a BET plot¹⁸ and the isotherm "B" point. If the BET equation is written in the form

$$\frac{P/P_o}{V_a(1 - P/P_o)} = \frac{1}{V_m C} + \frac{C - 1}{V_m C} \frac{P}{P_o} \quad (34)$$

it can be seen that from the slope and intercept of the plot P/P_o versus $\frac{P/P_o}{(1 - P/P_o)}$ the monolayer coverage can be determined, that is

$$V_m = \frac{1}{\text{slope} + \text{intercept}} \quad (35)$$

The isotherm "B", breakaway point is found by extrapolating back

along the straight line portion in the neighborhood of monolayer coverage. The point at which the extrapolation leaves the isotherm plot is known as the "B" point and the value of V_a at that point is taken as V_m .

Since the BET equation is based upon a model which does not fully correspond to the true behavior of the surface adsorption phenomena, and since the use of the isotherm "B" point is merely a guess at the value of the monolayer capacity, both methods previously described leave something to be desired.

CHAPTER IV

EXPERIMENTAL RESULTS

Multilayer isotherms for the krypton-boron nitride system were run at 71.44°K, 74.17°K, and 76.92°K. The volumes adsorbed, V_A , versus the equilibrium pressures are plotted in Figures 4-6. Monolayer isotherms for krypton on boron nitride, Figures 7 and 8, were run at 71.57°K, 73.76°K, and 77.01°K. The experimental isotherm data may be found in Appendix A. Monolayer isotherms for the krypton-graphite system were run at 74.56°K and 76.91°K. A θ versus P plot is shown in Figure 10, Chapter V, and the experimental isotherm data are given in Appendix A. The majority of points in both systems investigated represent both adsorption and desorption data thus assuring that a true equilibrium was attained in each case.

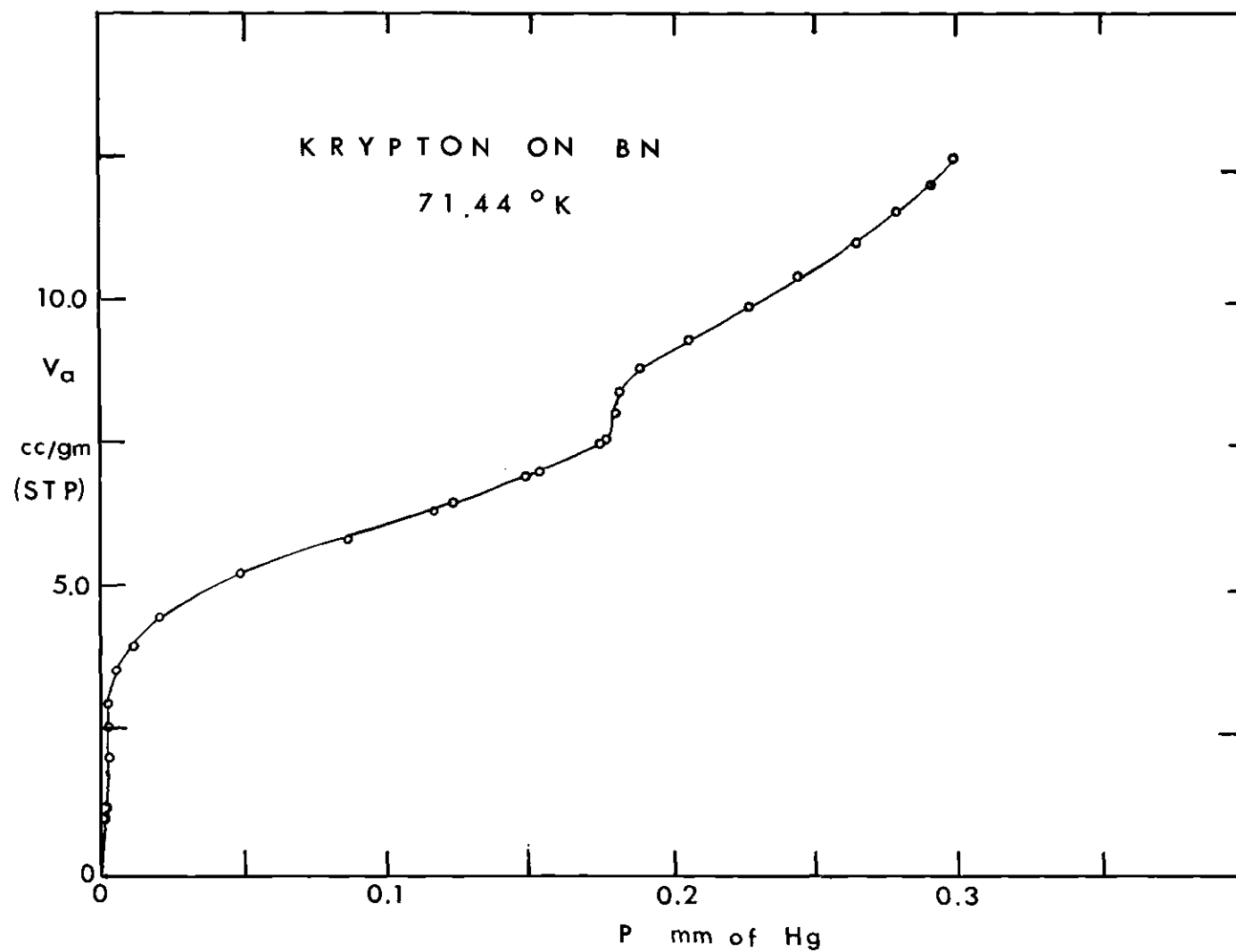


Figure 4. The Physical Adsorption of Krypton on Boron Nitride at 71.44 °K

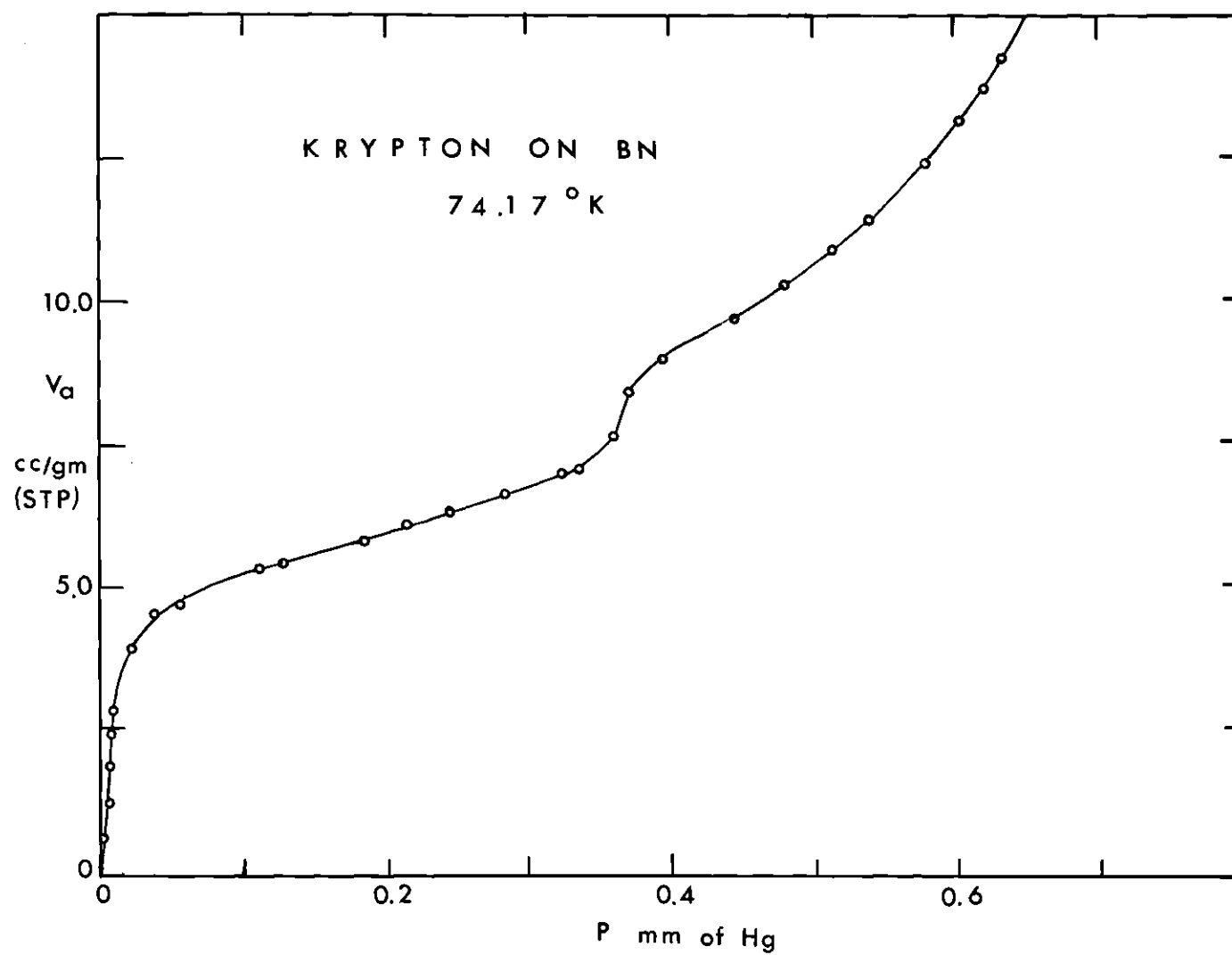


Figure 5. The Physical Adsorption of Krypton on Boron Nitride at 74.17 °K

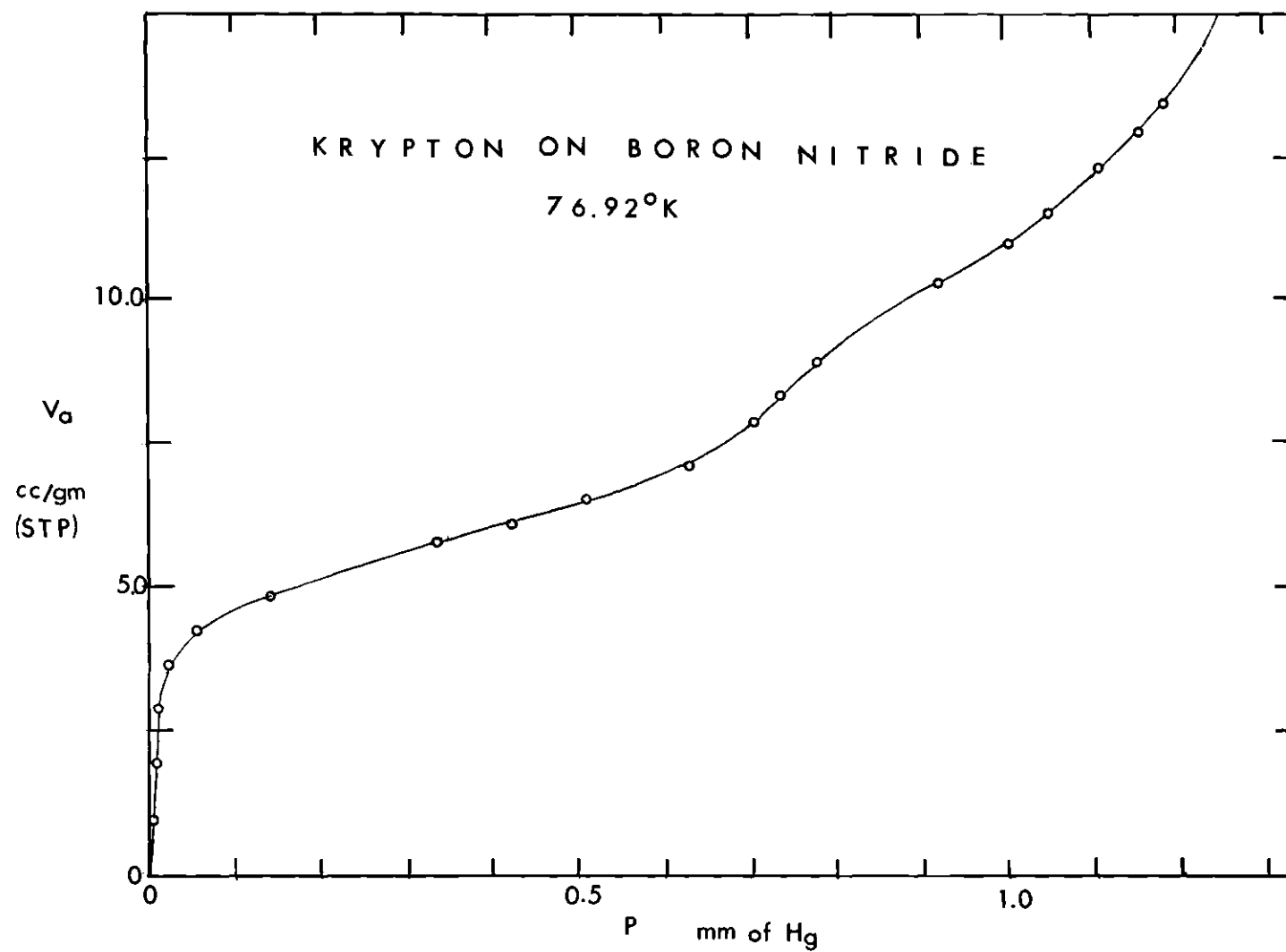


Figure 6. The Physical Adsorption of Krypton on Boron Nitride at 76.92 °K

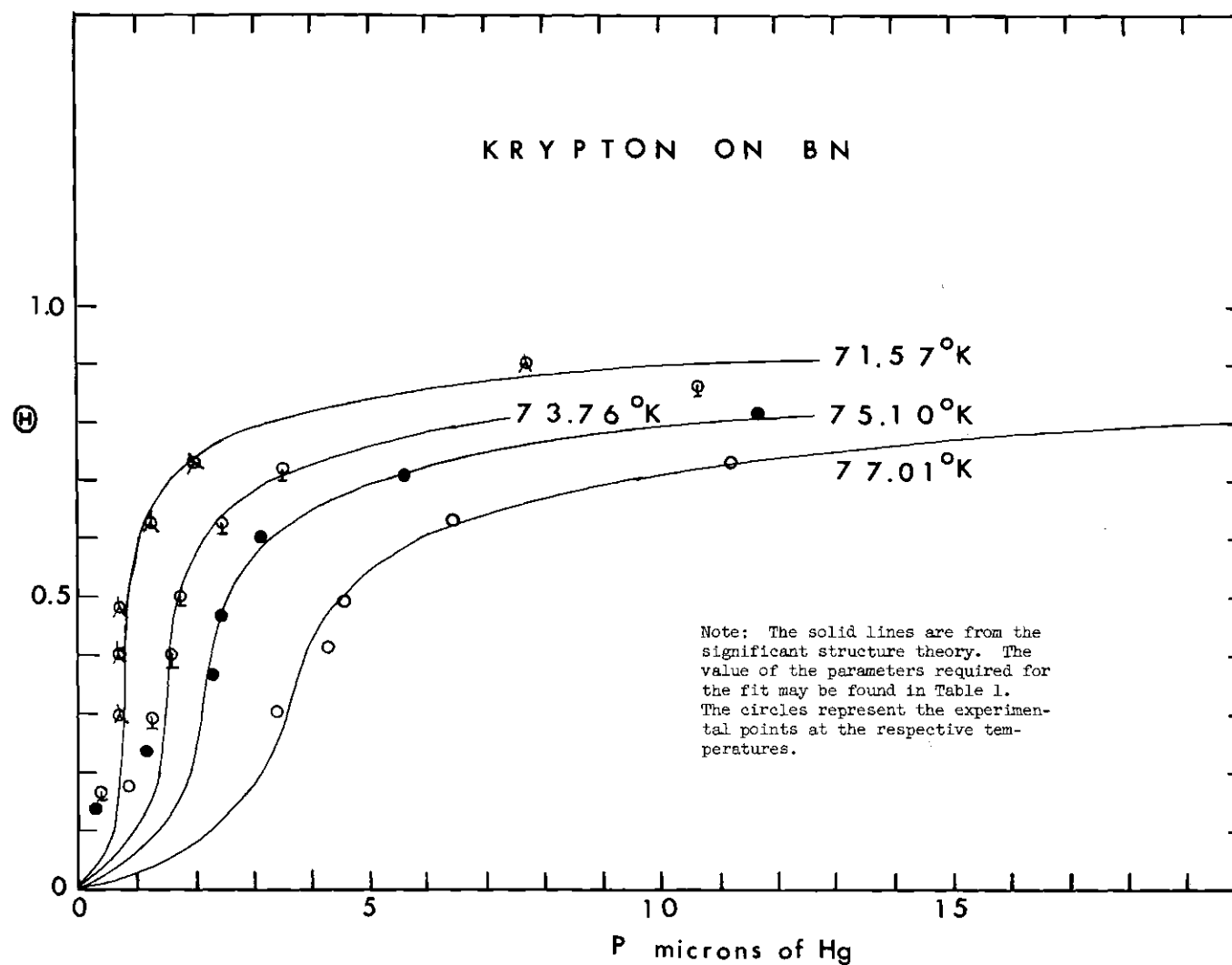


Figure 7. The Physical Adsorption of Krypton on Boron Nitride - Significant Structure Theory Fit to Experimental Data

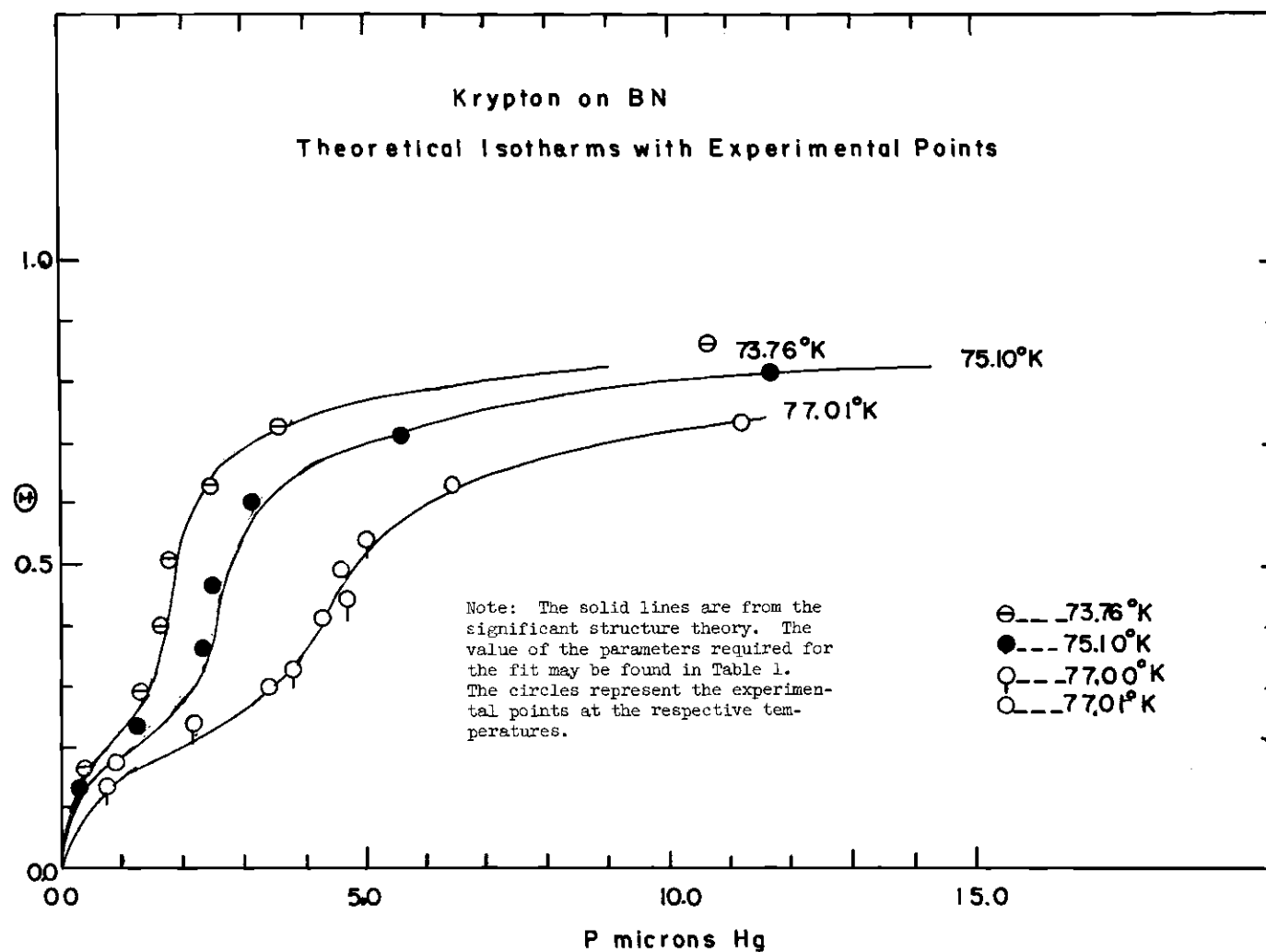


Figure 8. The Physical Adsorption of Krypton on Boron Nitride - Two Part Significant Structure Theory Fit to Experimental Data

CHAPTER V

DISCUSSION OF RESULTS

Krypton on Boron Nitride

The multilayer isotherms for this system are of the general shape expected and are remarkably similar to those of argon on boron nitride³⁶ in that the approximate position of the risers is the same in both systems: However, as can be seen from Figure 7, the sub-monolayer isotherms are a bit irregular in the region 0.0 θ to 0.20 θ .

At first the significant structure theory was applied to the data, Figure 7, and was found to give an excellent fit in the region 0.3 to 0.8 θ ; but, with great discrepancies below 0.2 θ . The high degree of purity of the boron nitride sample as indicated by x-ray diffraction would seem to minimize the possibility of errors introduced due to sample impurities. This would seem to indicate that the sample was either heterogeneous with a Gaussian distribution of adsorptive potentials among the adsorption sites or that there might possibly be two distinct types of adsorptive sites, a non-Gaussian distribution. The sharpness of the sub-monolayer riser would seem to eliminate the former possibility. Therefore, a non-Gaussian approach was carried through applying the significant structure theory to both portions of the surface, Figure 8. The resultant equation is given by

$$\theta(P) = (1 - \alpha) \theta_{ss}(P, U_{o1}) + \alpha \theta_{ss}(P, U_{o2}) \quad (36)$$

where α is the fraction of the surface consisting of sites with adsorptive potential U_{O_2} and θ_{ss} represents coverages determined from the significant structure theory. The values of the parameters required for the isotherm fits are given in Table 1.

The multilayer isotherm data were found to give a nice linear BET plot, Table 2, with a V_m value of 4.61 ± 0.06 cc/gm STP. The isosteric heat plot, Figure 9, was what might be expected with peaks in the neighborhood of unit layer coverage and approached the heat of sublimation of krypton at high coverage. The limiting value of the isosteric heats at zero coverage was found to be 2720 cal/mole ± 100 cal/mole.

To determine the characteristic mode of adsorption, localized or mobile, for the monolayer region, the experimental standard entropy changes for each model, columns two and three in Table 3, are compared to the theoretical values given beneath the experimental computations. Columns two and three are computed by means of equation (26) and the theoretical values by means of equations (30) and (32). It can be seen from the above comparison that the first layer is clearly mobile. Similar comparisons show the second layer also to be mobile.

One of the objectives of this work was to determine the two-dimensional critical temperature of krypton on boron nitride. Using the significant structure theory along with the experimental data, a value of $70.75^\circ\text{K} \pm 0.60^\circ\text{K}$ has been assigned to the major portion of the surface. It should be noted that there was clearly no evidence of two-dimensional condensation at 77.8°K as reported by Pultz² and Ross and Cripps.³

Table 1. Molecular Properties and Parameters for the Physical Adsorption of Krypton on Boron Nitride and Graphite

Boron Nitride

Significant Structure Theory Parameters

U_o cal/mole..... $2656^a \pm 6$	$A_m^o A^c/molecule.....19.5(78^\circ K)^c$
ϵ'/k °K..... $118^a \pm 1$	V_m cc/gm (STP)..... $4.61^a \pm 0.06$
ν_o sec ⁻¹ $1.00 \times 10^{12ba} \pm 0.02$	$T_c(2656)^\circ K.....70.75^a \pm 0.06$

Two Part Significant Structure Theory Parameters

(80% U_{o1} , 20% U_{o2})

U_{o1} cal/mole..... $2625^a \pm 6$	$A_m^o A^c/molecule.....19.5(78^\circ K)^c$
U_{o2} cal/mole..... $3000^a \pm 6$	V_m cc/gm (STP)..... $4.61^a \pm 0.06$
ν_o sec ⁻¹ $1.00 \times 10^{12ab} \pm 0.02$	$\alpha.....0.20^a$
ϵ'/k °K..... $118^a \pm 1$	T_c °K..... $70.75^a \pm 0.60$

Graphite

Significant Structure Theory Parameters

U_o cal/mole..... $2825^a \pm 6$	$A_m^o A^c/molecule.....19.5(78^\circ K)^c$
ϵ'/k °K..... $118^a \pm 1$	V_m cc/gm (STP)..... 2.86^d
ν_o sec ⁻¹ $1.00 \times 10^{12b} \pm 0.02$	T_c °K..... 70.75^{ae}

^aThis work

^bS. Ross, J. K. Saelens, and J. P. Olivier, *J. Phys. Chem.*, 66, 696 (1962)

^cA. Karnaukov, *Kinetika i Kataliz*, 3, 583 (1962)

^dJ. H. Singleton and G. D. Halsey, *J. Phys. Chem.*, 58, 1011 (1954)

^eInsufficient data to determine accurately

Table 2. BET Plot Data Points

T °K	76.92	74.17	71.44	Average
$\frac{\theta}{0.05}$				
0.05	0.0119	0.0115	0.0117	0.0117
0.10	0.0225	0.0220	0.0217	0.0221
0.15	0.0329	0.0322	0.0319	0.0323
0.20	0.0436	0.0430	0.0428	0.0431
0.25	0.0550	0.0547	0.0541	0.0546
0.30	0.0671	0.0670	0.0657	0.0666
0.35	0.0797	0.0798	0.0776	0.0790
$V_m \text{ cm}^3(\text{STP}) - \frac{\theta}{\text{gm}}$	4.59	4.55	4.72	4.61

Note: The numbers in columns 2, 3, 4, and 5 are equal to $\frac{P/P_o}{V_a(1 - P/P_o)}$

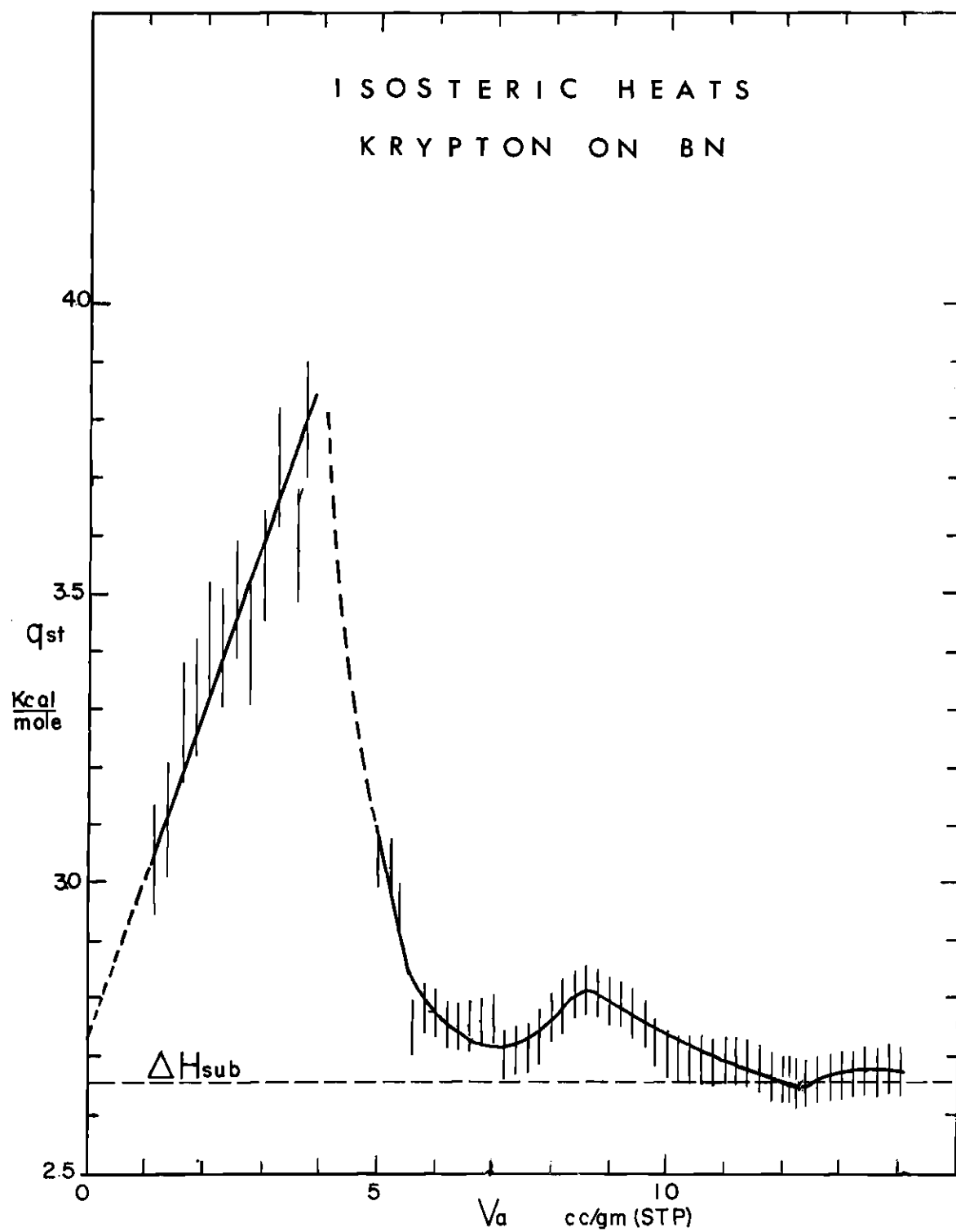


Figure 9. Isosteric Heats of Adsorption of Krypton on Boron Nitride at 75.10 °K

Table 3. Molar Integral Entropies of Adsorption
for Krypton on Boron Nitride

Monolayer Entropies at $T = 75.10^\circ\text{K}^*$

θ	$-\Delta S_a^\circ$	$-\Delta S_a^\circ$
	cal/mole localized	cal/mole mobile
0.30	17.22	8.73
0.40	16.22	9.65
0.50	17.20	10.18
0.60	18.75	10.70
0.70	20.78	10.20
0.80	23.16	10.17

$$S_{a, \text{tr}}^\circ = 21.40 \text{ cal/mole}$$

$$S_{g, \text{tr}}^\circ = 32.36 \text{ cal/mole}$$

$$-\Delta S_a^\circ = 32.36 \text{ cal/mole localized}$$

$$-\Delta S_a^\circ = 10.96 \text{ cal/mole mobile}$$

Multilayer Entropies at $T = 76.92^\circ\text{K}^{**}$

θ	$-\Delta S_a^\circ$	$-\Delta S_a^\circ$
	cal/mole localized	cal/mole mobile
1.30	19.97	13.99
1.40	19.43	12.84
1.50	18.64	11.57
1.60	17.74	9.65
1.70	17.41	7.64
1.80	17.02	3.97

$$S_{a, \text{tr}}^\circ = 21.47 \text{ cal/mole}$$

$$S_{g, \text{tr}}^\circ = 32.48 \text{ cal/mole}$$

$$-\Delta S_a^\circ = 32.48 \text{ cal/mole localized}$$

$$-\Delta S_a^\circ = 11.01 \text{ cal/mole mobile}$$

* The estimated error is ± 1.33 cal/mole $^\circ\text{K}$ for each entry.

** The estimated error is $\pm .67$ cal/mole $^\circ\text{K}$ for each entry.

Krypton on Graphite

The krypton-graphite system was also briefly investigated in the sub-monolayer region and the results evaluated by means of the significant structure theory, Figure 10, Table 1. The solid points in Figure 10 are experimental data points for a 74.9°K isotherm which was run by Pierotti⁶ a number of years prior to this work. The similarity of the 74.9°K isotherm of Pierotti and 74.76°K isotherm of this work would seem to lend support to the accuracy of the data. There was no evidence of two-dimensional condensation at 77.8°K as reported by Ross and Winkler.⁴ It should also be noted that the values of v_0 and ϵ'/k and, therefore, the critical temperatures were found to be the same for both the boron nitride and graphite systems. Although the adsorption parameters are expected to be slightly different for these two systems, they appear to be the same within the experimental error of the present methods.

Recommendations for Further Study

In view of the previously discussed findings concerning the krypton-boron nitride system, it is recommended that further work be conducted on the preparation and purification of boron nitride in order to obtain a more completely isotactic surface on which to run adsorption isotherms. It is also recommended that the significant structure theory as applied to physical adsorption on a homogeneous surface be extended to include multilayer adsorption. Finally, the findings of this work concerning the krypton-graphite system would seem to warrant further investigation into the determination of the two-dimensional critical temperature of the krypton-graphite system.

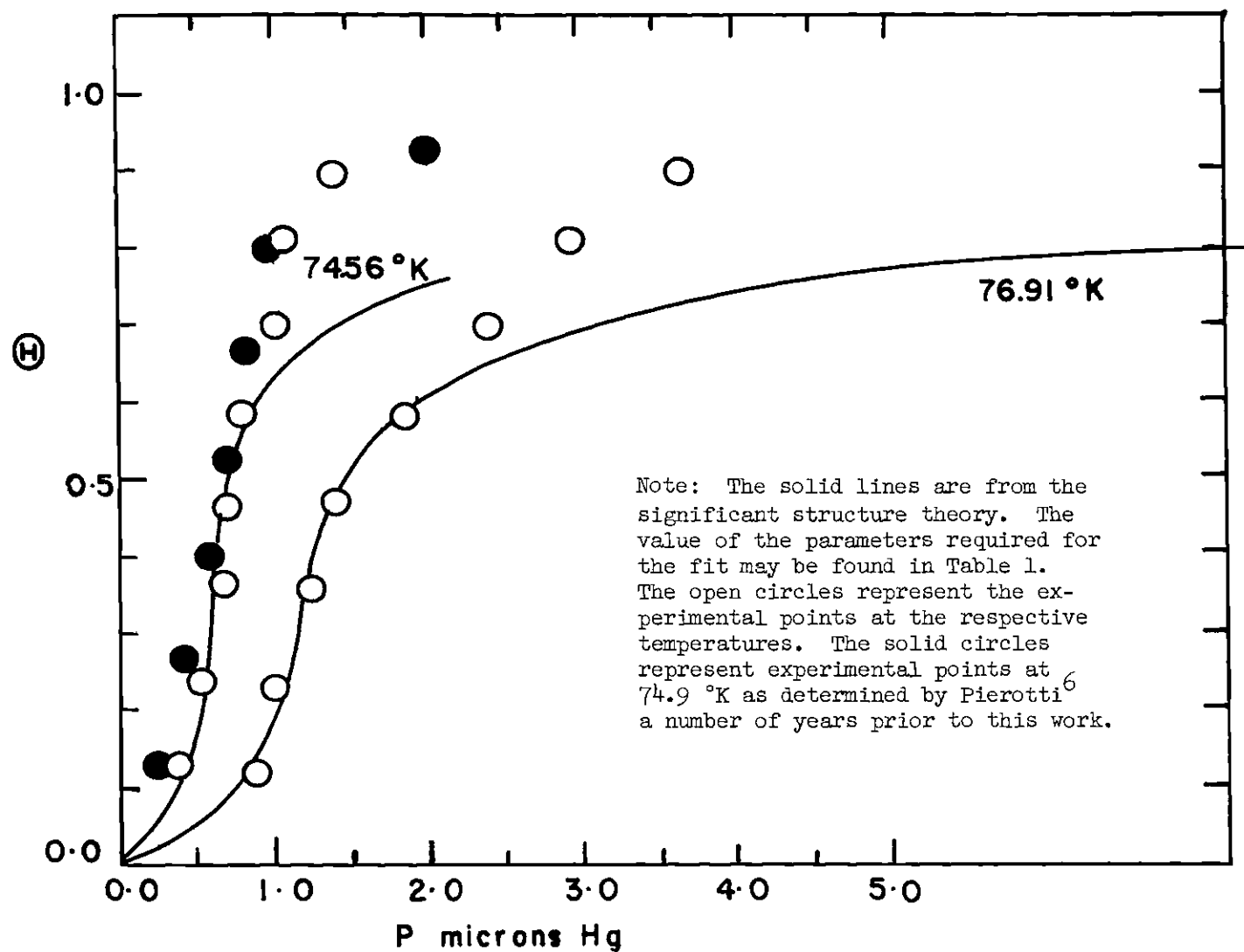


Figure 10. The Physical Adsorption of Krypton on Graphite - Significant Structure Theory Fit to Experimental Data

APPENDICES

APPENDIX A
EXPERIMENTAL DATA

Table 4. Multilayer Data for the Physical Adsorption
of Krypton on Boron Nitride at 76.92°K

$$P_0 = 1.59 \text{ mm of Hg}, V_m = 4.61 \text{ cm}^3(\text{STP})/\text{gm}$$

V_a $\text{cm}^3(\text{STP})/\text{gm}$	P mm of Hg	P/P ₀	θ	Isotherm Run No.
4.24	0.053	0.033	0.920	1
4.85	0.141	0.089	1.052	1
5.80	0.334	0.210	1.259	1
6.12	0.425	0.267	1.328	1
6.55	0.510	0.321	1.421	1
7.12	0.630	0.396	1.545	2
7.30	0.655	0.412	1.584	1
7.90	0.707	0.445	1.714	1
8.39	0.735	0.462	1.821	1
8.99	0.780	0.491	1.951	1
10.34	6.924	0.581	2.244	2
11.00	1.003	0.641	2.387	2
11.52	1.054	0.663	2.500	2
12.33	1.110	0.698	2.686	2
12.96	1.156	0.727	2.812	2
13.46	1.184	0.745	2.921	2
14.17	1.216	0.765	3.074	2
15.68	1.262	0.794	3.403	2
0.98	0.0052	0.0033	0.213	1
1.98	0.0092	0.0058	0.430	1
2.89	0.0126	0.0079	0.627	1
3.63	0.021	0.013	0.788	1

Table 5. Multilayer Data for the Physical Adsorption
of Krypton on Boron Nitride at 74.17°K
 $P_0 = 0.840$ mm of Hg, $V_m = 4.61$ cm³(STP)/gm

V_a cm ³ (STP)/gm	P mm of Hg	P/P ₀	θ	Isotherm Run No.
4.53	0.037	0.044	0.983	3
4.75	0.055	0.065	1.031	1
5.39	0.111	0.132	1.170	1
5.42	0.127	0.151	1.176	3
5.89	0.183	0.218	1.278	1
6.13	0.216	0.257	1.330	3
6.38	0.245	0.292	1.384	1
6.68	0.284	0.338	1.450	3
7.02	0.324	0.386	1.523	1
7.12	0.335	0.399	1.545	3
7.66	0.360	0.429	1.662	2
8.44	0.371	0.442	1.831	2
9.02	0.395	0.470	1.957	2
9.76	0.444	0.529	2.118	2
10.33	0.479	0.570	2.242	2
10.94	0.513	0.611	2.374	2
11.42	0.539	0.642	2.478	2
12.41	0.579	0.689	2.693	2
13.19	0.602	0.717	2.862	2
13.79	0.620	0.738	2.992	2
14.26	0.632	0.752	3.104	2
15.16	0.649	0.773	3.290	2
16.38	0.668	0.795	3.554	2
0.69	0.0028	0.0033	0.150	1
1.23	0.0054	0.0064	0.267	1
1.92	0.0064	0.0076	0.417	1
2.46	0.0064	0.0076	0.534	1
2.89	0.0081	0.0096	0.627	1
3.93	0.0203	0.024	0.853	1

Table 6. Multilayer Data for the Physical Adsorption
of Krypton on Boron Nitride at 71.44°K
 $P_o = 0.427$ mm of Hg, $V_m = 4.61$ cm³(STP)/gm

V_a cm ³ (STP)/gm	P mm of Hg	P/P _o	θ	Isotherm Run No.
4.47	0.020	0.047	0.970	1
5.23	0.048	0.112	1.135	1
5.86	0.086	0.201	1.272	1
6.37	0.116	0.272	1.382	1
7.02	0.154	0.361	1.523	1
7.60	0.177	0.415	1.649	1
6.50	0.123	0.288	1.411	3
6.95	0.149	0.349	1.508	3
7.52	0.175	0.410	1.632	3
8.05	1.800	0.422	1.747	3
8.48	0.182	0.426	1.840	3
8.82	0.189	0.453	1.910	3
9.38	0.206	0.482	2.035	3
9.91	0.227	0.532	2.150	3
10.45	0.244	0.571	2.268	3
11.03	0.265	0.621	2.394	3
11.60	0.279	0.653	2.517	3
12.07	0.291	0.681	2.619	3
12.50	0.209	0.700	2.713	3
12.84	0.304	0.712	2.786	3
13.12	0.308	0.721	2.847	3
13.55	0.313	0.733	2.940	3
14.08	0.320	0.749	3.055	3
0.98	0.0012	0.0028	0.213	1
1.11	0.0015	0.0035	0.241	2
2.02	0.0020	0.0046	0.438	2
2.54	0.0020	0.0046	0.552	2
2.96	0.0019	0.0045	0.642	2
3.52	0.0053	0.0124	0.764	2
3.98	0.107	0.025	0.864	2

Table 7. Monolayer Data for the Physical Adsorption
of Krypton on Boron Nitride
 $V_m = 4.61 \text{ cm}^3(\text{STP})/\text{gm}$

T °K	77.01		77.00		75.10	
	θ	P	θ	P	θ	P
		microns Hg		microns Hg		microns Hg
	0.174	0.87	0.134	0.70	0.133	0.26
	0.308	3.38	0.240	2.11	0.236	1.18
	0.415	4.28	0.322	3.79	0.368	2.29
	0.495	4.55	0.444	4.68	0.470	2.41
	0.631	6.42	0.541	4.94	0.603	3.09
	0.738	11.22			0.710	5.57
					0.817	11.69

T °K	73.76		71.57	
	θ	P	θ	P
		microns Hg		microns Hg
	0.166	0.35	0.168	0.35
	0.294	1.26	0.299	0.66
	0.400	1.59	0.404	0.65
	0.508	1.73	0.484	0.68
	0.630	2.44	0.623	1.18
	0.726	3.51	0.730	1.97
	0.867	10.62	0.904	7.72

Table 8. Monolayer Data for the Physical Adsorption
of Krypton on Graphite
 $V_m = 2.86 \text{ cm}^3(\text{STP})/\text{gm}$

T °K				
θ		P microns Hg	θ	P microns Hg
0.120		0.85	0.134	0.34
0.232		0.97	0.239	0.51
0.366		1.24	0.368	0.68
0.472		1.40	0.471	0.70
0.584		1.83	0.592	0.84
0.703		2.42	0.705	0.99
0.814		2.95	0.819	1.03
0.902		3.65	0.955	1.39

APPENDIX B
ISOSTERIC HEAT COMPUTATIONS AND ERROR ANALYSIS

APPENDIX B

ISOSTERIC HEAT COMPUTATIONS AND ERROR ANALYSIS

The isosteric heats were determined through the use of equations 14 through 17. The errors in the multilayer isosteric heats were estimated by taking the isotherms in pairs and integrating the equation

$$(\mathrm{d} \ln P / \mathrm{d} T)_{\theta} = q_{\mathrm{st}} / RT^2$$

over the appropriate limits. Since three multilayer isotherms were run, three different pairs were used to determine three values for q_{st} . The average deviation was found to be ± 50 cal/mole.

The bulk of this error was attributed to the processes of plotting, curve drawing, and interpolation. As one can see, in the multilayer region the isotherms crossed the constant θ lines at fairly acute angles. The result was about a two percent error in extracting pressure readings from the graph at a given value of θ .

The computed error in the isosteric heats may be justified in the following manner.

To evaluate the isosteric heats the equation

$$q_{\mathrm{st}} = R[T_1 T_2 / (T_2 - T_1)] [\ln(P_2 / P_1)]$$

may be used where q_{st} is taken as independent of temperature.

Now the error in temperature measurement is negligible, approximately 0.05 percent, thus, the bulk of the error is in the term $\ln(P_2/P_1)$.

If a RMS error method is used, the percent error in $\ln(P_2/P_1)$ is given by

$$\sqrt{(\% \text{ error } P_1)^2 + (\% \text{ error } P_2)^2} = \%E$$

Therefore, the accuracy of the isosteric heats is given by

$$q_{st} = R[T_1T_2/(T_2 - T_1)] \ln[(P_2/P_1)(1 \pm \%E)]$$

Now, when $\%E$ is small compared to one,

$$\ln[(P_2/P_1)(1 \pm \%E)] = \ln(P_2/P_1) + \%E$$

and the error in the isosteric heats is estimated by

$$R[T_1T_2/(T_2 - T_1)] (\pm \%E)$$

From the above equation, one can see that the two percent error in pressure due to plotting and curve drawing produced a ± 50 cal/mole error in the isosteric heats.

The error in pressure measurement in the multilayer region of 0.3 percent produced an error of only ± 7 cal/mole.

In the monolayer region, the error was determined to be ± 100 cal/mole. In this instance the error due to plotting and curve drawing

was about ± 0.5 percent, thereby producing a ± 12 cal/mole error in the isosteric heats. The balance of the isosteric heat error was due to about a two percent error in pressure measurement at five microns total pressure and five percent at two microns total pressure.

Table 9. Monolayer Isosteric Heats of Adsorption for the Krypton-Boron Nitride System at 75.10 °K

V_a $\text{cm}^3(\text{STP})/\text{gm}$	q_{st} Kcal/mole
1.15	3.031
1.38	3.101
1.61	3.271
1.84	3.313
2.08	3.409
2.31	3.401
2.54	3.478
2.77	3.401
3.00	3.535
3.23	3.710
3.59	3.566
3.69	3.792

Table 10. Multilayer Isosteric Heats of Adsorption for the
Krypton-Boron Nitride System at 76.92 °K

V_a $\text{cm}^3(\text{STP})/\text{gm}$	q_{st} Kcal/mole	V_a $\text{cm}^3(\text{STP})/\text{gm}$	q_{st} Kcal/mole
5.00	3.034	9.20	2.793
5.20	3.028	9.40	2.776
5.40	2.959	9.60	2.758
5.60	2.745	9.80	2.727
5.80	2.786	10.00	2.706
6.00	2.774	10.20	2.698
6.20	2.758	10.40	2.695
6.40	2.753	10.60	2.693
6.60	2.752	10.80	2.691
6.80	2.762	11.00	2.697
7.00	2.763	11.20	2.693
7.20	2.702	11.40	2.689
7.40	2.714	11.60	2.680
7.60	2.715	11.80	2.691
7.80	2.739	12.00	2.661
8.00	2.765	12.20	2.658
8.20	2.784	12.40	2.658
8.40	2.806	12.60	2.663
8.60	2.816	12.80	2.669
8.80	2.810	13.00	2.672
9.00	2.799	13.20	2.671
		13.40	2.675
		13.60	2.676
		13.80	2.677
		14.00	2.676

APPENDIX C

SIGNIFICANT STRUCTURE THEORY COMPUTATIONS AND ERROR ANALYSIS

APPENDIX C

SIGNIFICANT STRUCTURE THEORY COMPUTATIONS AND ERROR ANALYSIS

To determine U° , ϵ'/k , and v_{\circ} , equation 1 was programmed to give p at a number of predetermined θ values and a designated set of U_{\circ} , ϵ'/k , v_{\circ} and T values. The quantities ϵ'_{\circ} and A_m° were taken as six and 19.5 $A^{\circ 2}$ /molecule, respectively.

The process of fitting the isotherms was accomplished by first varying ϵ'/k to obtain the correct slope and then varying U_{\circ} and v_{\circ} to obtain the final fit to the set of isotherms.

Where more than one type of adsorptive site was involved in the same isotherm, equation 36 was used in conjunction with equation 1 to obtain the fit.

The maximum possible error in U_{\circ} was estimated to be ± 6 cal/mole in the following manner.

v_{\circ} and ϵ'/k were assumed to be correct as determined. Therefore, the error in the isotherm fits was approximated by

$$(1 \pm \% \text{ error}) = \exp (\Delta U_{\circ}/RT)$$

where ΔU_{\circ} was the error in U_{\circ} .

At an average error in the isotherm fits of four percent at a temperature of 75°K, the error in U_{\circ} was found to be ± 6 cal/mole.

Table 11. Significant Structure Theory Computations for the Krypton-Boron Nitride System at Various Temperatures
 $U_o = 2656$ cal/mole, $\epsilon_o'/k = 118^\circ\text{K}$, $\nu_o = 1.00 \times 10^{12}$ sec^{-1} , and $A_m^o = 19.5 \text{ Å}^2/\text{molecule}$. (Graphical representation of these computations may be found in Figure 9.)

T °K	77.01	75.10	73.76	71.57
θ	P microns Hg	P microns Hg	P microns Hg	P microns Hg
0.1	2.26	1.40	0.99	0.54
0.2	3.15	1.91	1.33	0.71
0.3	3.54	2.10	1.43	0.74
0.4	3.88	2.25	1.51	0.76
0.5	4.50	2.55	1.68	0.82
0.6	5.89	3.26	2.11	1.01
0.7	9.52	5.15	3.29	1.52
0.8	22.00	11.63	7.29	3.27
0.9	99.34	51.34	31.65	13.79

Table 12. Significant Structure Theory Computations for the Krypton-Boron Nitride System at Various Temperatures

$U_o = 2625$ cal mole, $\epsilon'/k = 118$ °K, $v_o = 1.00 \times 10^{12}$ sec⁻¹, $A_m^o = 19.5$ Å²/molecule

T °K	77.01	75.10	73.76
θ	P microns Hg	P microns Hg	P microns Hg
0.1	2.75	1.72	1.22
0.2	3.84	2.35	1.64
0.3	4.32	2.58	1.76
0.4	4.73	2.76	1.87
0.5	5.49	3.13	2.07
0.6	7.18	4.00	2.60
0.7	11.6	6.33	4.06
0.8	26.8	14.3	8.99
0.9		63.1	38.99

Table 13. Significant Structure Theory Computations for the Krypton-Boron Nitride System at Various Temperatures

$U_o = 3000 \text{ cal/mole}$, $\epsilon'/k = 118 \text{ }^\circ\text{K}$, $\nu_o = 1.00 \times 10^{12} \text{ sec}^{-1}$, $A_m^o = 19.5 \text{ A}^2/\text{molecule}$

T $^\circ\text{K}$	77.01	75.10	73.76	71.57
θ	P microns Hg	P microns Hg	P microns Hg	P microns Hg
0.1	0.238	0.140	0.095	0.049
0.2	0.333	0.191	0.127	0.063
0.3	0.374	0.210	0.137	0.066
0.4	0.410	0.224	0.144	0.068
0.5	0.475	0.254	0.161	0.073
0.6	0.622	0.325	0.202	0.090
0.7	1.005	0.514	0.314	0.135
0.8	2.320	1.160	0.698	0.291
0.9	10.490	5.120	3.030	1.230

Table 14. Significant Structure Theory Computations for the Krypton-Boron Nitride System at Various Temperatures Assigning an Adsorptive Potential of 2625 cal/mole to Eighty Percent of the Surface and 3000 cal/mole to the Remaining Twenty Percent.
 $\epsilon'_0/k = 118^\circ\text{K}$, $\nu_0 = 1.00 \times 10^{12} \text{ sec}^{-1}$, $A_m^0 = 19.5 \text{ \AA}^2/\text{molecule}$. Graphical representation of these computations may be found in Figure 8.

T °K	77.01		75.10		73.76	
	θ	P microns Hg	θ	P microns Hg	θ	P microns Hg
	0.108	0.47	0.108	0.25	0.128	0.20
	0.156	1.01	0.156	0.51	0.195	0.70
	0.218	2.32	0.200	1.16	0.298	1.50
	0.293	3.50	0.276	2.00	0.364	1.70
	0.393	4.25	0.380	2.50	0.465	1.85
	0.490	4.70	0.490	2.75	0.554	2.00
	0.546	5.20	0.550	3.00	0.650	2.50
	0.604	6.00	0.658	4.00	0.692	3.03
	0.662	7.50	0.810	11.0	0.782	5.50
	0.727	10.5	0.830	14.3	0.826	9.00
	0.742	11.6				

Table 15. Significant Structure Theory Computations for the Krypton-Graphite System at Various Temperatures
 $U_0 = 2825$ cal/mole, $\epsilon'/k = 118$ °K, $v_0 = 1.00 \times 10^{12}$ sec⁻¹, $A_m^0 = 19.5$ Å²/molecule. (Graphical representation of these computations may be found in Figure 10.)

T °K	76.91	74.56
θ	P microns Hg	P microns Hg
0.1	0.730	0.391
0.2	1.02	0.528
0.3	1.14	0.577
0.4	1.25	0.613
0.5	1.45	0.690
0.6	1.89	0.877
0.7	3.05	1.387
0.8	7.05	3.09
0.9	31.78	13.53

BIBLIOGRAPHY

1. J. H. de Boer, Advan. Colloid Sci., III, 3, 1950
2. W. W. Pultz, Dissertation Abstr. 20, 525 (1959)
3. S. Ross and J. P. Olivier, "On Physical Adsorption," Interscience Publishers, New York, N. Y., 1964, p. 226
4. S. Ross and W. Winkler, J. Colloid Sci., 10, 330 (1955)
5. H. Clark, J. Phys. Chem., 59, 1068, (1955)
6. R. A. Pierotti, unpublished work
7. J. H. Singleton and G. D. Halsey, Jr., J. Phys. Chem., 58, 1011 (1954)
8. I. Langmuir, J. Am. Chem. Soc., 39, 1848, (1917)
9. S. Ross and J. P. Olivier, "On Physical Adsorption," Interscience Publishers, New York, N. Y., 1964, p. 8
10. I. Langmuir, J. Am. Chem. Soc., 38, 2267 (1916); Ibid., 40, 1361 (1918); Phys. Rev., 8, 149, (1916)
11. R. H. Fowler and E. A. Guggenheim, "Statistical Thermodynamics," Cambridge University Press, Cambridge, Mass., 1949, p. 431
12. S. Ross and J. P. Olivier, "On Physical Adsorption," Interscience Publishers, New York, N. Y., 1964, p. 160
13. Ibid., p. 159
14. J. H. de Boer, "The Dynamical Character of Adsorption," Clarendon Press, Oxford, 1953, p. 17
15. J. J. McAlpin and R. A. Pierotti, J. Chem. Phys., 41, 68 (1964)
16. J. J. McAlpin and R. A. Pierotti, J. Chem. Phys., 42, 1842 (1965)
17. H. Eyring, T. Ree, and N. Hirai, Proc. Natl. Acad. Sci. U. S., 44, 683 (1958)

Note: The abbreviations used here follow the form employed by Chemical Abstracts (see Vol. 55, Part 9, p. 1J).

BIBLIOGRAPHY

18. S. Brunauer, P. H. Emmett, and E. Teller, J. Am. Chem. Soc., 60, 309 (1938)
19. T. L. Hill, J. Chem. Phys., 15, 767 (1947)
20. W. M. Champion and G. D. Halsey, Jr., J. Phys. Chem., 57, 646 (1953)
21. J. H. Singleton and G. D. Halsey, Jr., Can. J. Chem., 33, 184 (1954)
22. R. A. Pierotti, J. Phys. Chem., 68, 1810 (1962)
23. J. H. Singleton and G. D. Halsey, Jr., J. Phys. Chem., 58, 330 (1954)
24. F. W. Lytle and J. T. Stoner, Science, 148, 1721 (1965)
25. S. Weber, Commun. Phys. Lab. Univ. Leiden, No. 246b (1937)
26. G. A. Miller, J. Phys. Chem., 67, 1359 (1963)
27. Landolt-Bornstein, "Zahlenwerte und Funktionen," Sections 13 241 and 13 242, Springer-Verlag, Berlin, 1940-1951
28. A. F. Devonshire, Proc. Roy. Soc. (London), Ser. A 163, 132, 1937
29. S. Ross and J. P. Olivier, "On Physical Adsorption," Interscience Publishers, New York, N. Y., 1964, pp. 123-136
30. Ibid., pp. 117-118
31. Ibid., p. 154
32. Ibid., p. 156
33. Ibid., p. 158
34. J. H. de Boer and S. Kruyer, Koninkl. Ned. Akad. Wetenschap. Proc., 55B, 451 (1952); 56B, 67, 236, 415 (1953); 57B, 92 (1954); 58B, 61 (1955)